"In presenting the dissertation as a partial fulfillment of the requirements for an advanced degree from the Georgia Institute of Technology, I agree that the Library of the Institution shall make it available for inspection and circulation in accordance with its regulations governing materials of this type. I agree that permission to copy from, or to publish from, this dissertation may be granted by the professor under whose direction it was written, or such copying or publication is solely for scholarly purposes and does not involve potential financial gain. It is understood that any copying from, or publication of, this dissertation which involves potential financial gain will not be allowed without written permission.

AN INVESTIGATION OF FACTORS AFFECTING THE VISCOSITIES OF SOLID-LIQUID SUSPENSIONS

A THESIS

Presented to

The Faculty of the Graduate Division

Georgia Institute of Technology

In Partial Fulfillment

of the Requirements for the Degree

Master of Science in Mechanical Engineering

By

Harold Glenn Blocker

June 1954

AN INVESTIGATION OF FACTORS AFFECTING

THE VISCOSITIES OF SOLID-LIQUID SUSPENSIONS

Approved:

Date Approved by Chairman: June 4, 1954

ACKNOWLEDGEMENTS

The author wishes to acknowledge the contributions to this work and to express his appreciation to the following individuals: to Dr. J. M. DallaValle for suggesting the thesis problem and methods for its solution; to Dr. Clyde Orr, Jr., who not only offered many helpful suggestions and criticizms but also made the settling volume measurements and helped design and build the viscometer; and to Drs. M. J. Goglia and W. B. Harrison for carefully reading and criticizing the manuscript.

TABLE OF CONTENTS

(Continued)

TABLE OF CONTENTS (Continued)

LIST OF TABLES

LIST OF FIGURES

(Continued)

LIST OF FIGURES (Continued)

AN INVESTIGATION OF FACTORS AFFECTING THE VISCOSITIES OF SOLID-LIQUID SUSPENSIONS

Harold Glenn Blocker

SUMMARY

The purpose of this investigation was to develop a method for predicting the viscosities of solid-liquid suspensions from well-known or easily-determinable properties of the component materials. Many expressions have been suggested by previous investigators with which to describe data for specific systems within certain limits, however, certain factors of obvious importance, such as the particle size distribution and shape and the attractive forces between particles, are seldom considered. A few of the more recent investigators considered these factors indirectly and their work suggested the correlation attempted in this study.

The viscosities of a number of solid-liquid suspensions were measured in a capillary tube viscometer made by modifying a commercial viscometer. Properties of the suspension and of its components which were expected to affect the viscosities of the suspensions were evaluated. The flow characteristics of the suspensions investigated were analyzed by the use of shear diagrams.

It was found that most of the suspensions used in this investigation were approximately Newtonian except at the highest concentrations. For these conditions it was concluded that the viscosities of

such suspensions could be predicted with moderate accuracy without recourse to experimental viscosity measurements by means of the empirical equation

$$\mu_o/\mu = (1 - C/C_s)^{\sigma} ,$$

where μ_o is the viscosity of the liquid medium, μ is the viscosity of the suspension, C is the fraction of the total volume occupied by the solid particles, C_s is the fraction of the total volume occupied by the solid particles in a bed formed by sedimentation from the suspension and σ is the geometric standard deviation obtained from particle size analysis. A more accurate indication of viscosity may be obtained by use of the equation

$$\mu_o/\mu = (1 - C/C_s)^{k} ,$$

where the value of the constant k is determined from one or more viscosity measurements and the other terms are as described above.

CHAPTER I

INTRODUCTION

The flow of finely-divided solid materials suspended in liquid media is very important in modern engineering. The pipeline transportation and pumping characteristics of suspensions, or slurries, of sand, paper pulp and coating clays provide important examples. The wide-spread handling of such suspensions requires a knowledge of the viscosity characteristics of these materials. Frequently, nowever, time does not permit and the need does not justify an extensive investigation of these characteristics. While many expressions have been suggested by previous investigators to describe data for specific systems over certain limits, no generalized relationship has been developed by which the viscosity of a suspension at any given set of conditions can be predicted with assurance. Therefore, this investigation was initiated in order to provide a method for predicting the viscosities of solid-liquid suspensions from well-known or easily-determinable properties of the component materials.

Suspensions of solid particles are classified into two general types according to the dependence of the viscosity, or apparent viscosity, on the rate of shear during laminar flow. A fluid is said to be Newtonian when its viscosity is independent of the rate of shear, i.e., when it exhibits a linear shear-shearing stress relationship passing through the origin as shown in the shear diagram, Figure 1. A shear

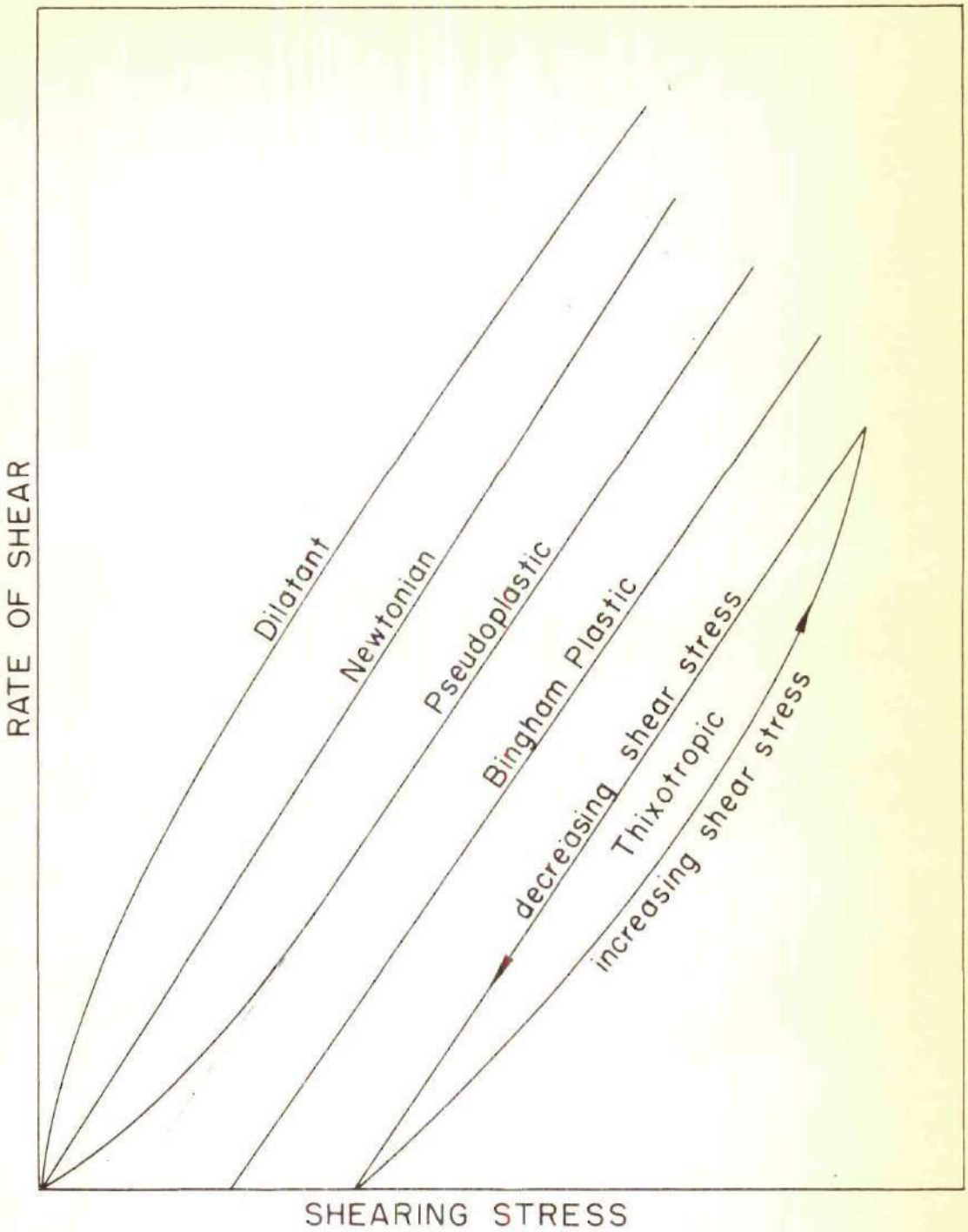

Figure 1. Shear Diagrams for Newtonian and Non-Newtonian Suspensions. Thixotropic Diagram Shows Hysteresis Loop.

diagram is a plot of the rate of shear versus the shearing stress. For Newtonian fluids, the inverse slope of this line is constant and equals the viscosity of the fluid.

All fluids which do not satisfy the above requirements are said to be non-Newtonian. They have been further classified by Alves (1949), for example, into five general types, viz., (1) Bingham plastics, (2) pseudoplastic, (3) dilatant, (4) thixotropic and (5) rheopectic. Typical shear diagrams of the first four types are illustrated in Figure 1. It will be noted that the apparent viscosity of a thixotropic suspension is dependent not only on the shearing stress, but also on the history of the suspension, i.e., with the duration of the flow. Rheopectic suspensions are certain thixotropic suspensions which will "set", or increase rapidly in apparent viscosity, upon being rythmically shaken or tapped.

Almost all pure liquids and many dilute suspensions are Newtonian in character. Concentrated suspensions, however, are usually non-Newtonian, their viscosities varying not only with temperature and composition, as do the viscosities of dilute suspensions, but also with rate of shear and in some cases with the duration of shear. This means that the apparent viscosity of a suspension may depend on the physical dimensions of the system in which it will be used and on the velocity of flow in the system. It also means that the viscosity of the suspension may differ at various levels within a pipeline, for example. At certain flow rates and concentrations, the suspension may take on entirely different flow characteristics. An analysis of the situation in the light of the liquid's motion and the behavior of particles suspended in the

liquid has been considered by Bingham (1922) and by Orr (1952).

Many expressions have been suggested by previous investigators to describe data for specific systems within certain limits. A few of the more important relationships, those that exhibit the general forms to be found, will be cited.

One of the best-known formulas for dilute suspensions was presented almost fifty years ago by Einstein (1906, 1911). The relationship is

$$\mu = \mu_o(1 + 2.5C) \ , \qquad (1)$$

where μ is the viscosity of the suspension, μ_o the viscosity of the liquid phase at the same temperature and C is the fraction of the total volume occupied by the solid particles. This is a theoretical equation based on the assumptions that the particles are spherical, uncharged, large in comparison with the liquid molecules and comprise a small fraction of the total volume, that there is no slip between the particles and the liquid and that turbulence is avoided. The equation describes experimental results at low concentrations but fails at concentrations over a few per cent. Eirich, Bunzl and Margaretha (1936) confirmed the equation for spheres at concentrations up to five or ten per cent, depending on the instrument used. McBain (1950) cites cases where values of the constant of 10 and 35 instead of 2.5 are required. Hatschek (1913) proposed a similar equation with a theoretical value of 4.5 instead of 2.5. Again, experimental confirmation can generally be obtained only with dilute suspensions.

Later, Hatschek (1920) proposed the relationship

$$\mu = \mu_o/(1 - C^{1/3}) \qquad (2)$$

for emulsions and used the results of measurements made on a suspension of red blood corpuscles to justify his relationship. This equation was derived for elastically deformable particles comprising more than half of the suspension's volume. It would seem to be an inappropriate choice for rigid particles, but it actually describes many suspension data better than other equations. Bonilla, et al. (1951) used this equation satisfactorily to give the viscosity of relatively dilute water-chalk suspensions in a heat transfer study.

Vand (1948) developed the theoretical relationship

$$\mu = \mu_o(1 + 2.5C + 7.17C^2 + 16.2C^3) \ . \qquad (3)$$

His results for glass spheres in a saturated solution of zinc iodide and in a mixture of water and glycerine fitted the relationship reasonably well up to concentrations of 25 volume per cent. As far as this author knows, no confirmation of Equation 3 has been obtained with irregular particles. Guth and Simha (1936) also expressed the viscosity as a function of a power series of the volume concentration of suspended solid material.

Norton, Johnson and Lawrence (1944) developed the equation

$$\mu = \mu_o(1 - C) + aC + bC^d \ , \qquad (4)$$

where a, b and d are constants, which they found to express the viscosities of clay suspensions to high concentrations. This equation is the result of one of the most successful attempts thus far to describe the

viscosities of suspensions over a wide range of concentrations. However, the three empirical constants must be evaluated for each system, and the equation is not practical for many applications.

The viscosity of the liquid and the concentration of the solid phase are not the only factors affecting the viscosity of a suspension. In addition, the size distribution, shape and attractive forces of the particles should affect the viscous properties, but they are seldom considered. While not taken directly into account, the relationships found by Bingham and Durham (1911), Robinson (1949) and Orr and Dalla-Valle (1954) are dependent on these factors. Since the work of these investigators suggested the correlation to be presented below, a brief review of their work will be presented.

Bingham and Durham found that the fluidity of a suspension, i.e., the reciprocal of the viscosity, decreased linearly with increased solid concentration so that, if extrapolated, a fluidity of zero was indicated at rather low concentrations. The concentration at "zero fluidity" was found to be independent of temperature. Hence, at low concentrations, the fluidity could be expressed by

$$F = F_o(1 - C/C_o) , \tag{5}$$

where F is the fluidity of the suspension, F_o the fluidity of the liquid phase at the same temperature and C_o the fraction of solids at "zero fluidity". This equation may be expressed in terms of viscosity by the relationship

$$\mu_o/\mu = 1 - C/C_o . \tag{6}$$

If the value of C_o is known, this equation expresses the viscosities of dilute suspensions with considerable accuracy.

Robinson (1949) derived an expression that was based on assumptions similar to those of Einstein with the added concept that specific viscosity is not only proportional to the volume concentration, but is also inversely proportional to the volume of free liquid in the suspension. This concept is not unique, but the definition of "free liquid" is new. Robinson reasoned that the effective volume of the suspended particles is the packed sediment volume, i.e., the volume occupied by the bed formed by sedimentation of the particles from the suspension whose viscosity is being considered. The remainder of the volume is the volume of "free liquid". Using these assumptions, Robinson derived the relationship

$$(\mu - \mu_o)/\mu_o = kC/(1 - SC) , \qquad (7)$$

where k is a constant and S is the relative sediment volume, defined as the volume of the sedimented bed per unit volume of solid particles.

Orr and DallaValle (1954) have presented an empirical relationship including features of the relationships of Bingham and Durham and of Robinson. The relationship may be expressed as

$$\mu_o/\mu = (1 - C/C_s)^{1.8} , \qquad (8)$$

where C_s is the fraction of the solid component of a bed formed by gravity sedimentation from the liquid suspension. As may be readily seen, C_s is the reciprocal of S and the similarity of Equation 8 to Equations 6 and 7 is apparent.

CHAPTER II

APPARATUS

Selection of the Viscometer.--Viscosity measurements of suspensions are generally complicated by the fact that agitation must be provided in order to keep the particles in the suspension. The problem is, therefore, to provide a measuring device with a stirring mechanism which does not affect the viscosity measurements appreciably and with adequate temperature control. Rotating cup viscometers are not well-suited for such measurements when heavy suspended particles are used, because the agitation necessary to keep the particles in suspension would invalidate most measurements. The U. S. Bureau of Standards developed a simple viscometer with one multipaddle stirrer and a capillary discharge tube. It is described in more detail by DallaValle (1948). The apparatus used in this investigation was based on the same principle but included a number of refinements.

Description of the Viscometer.--A commercial Saybolt viscometer manufactured by the Portable Products Corporation, C. J. Tagliabue Division, Brooklyn, New York, was modified and used as the main component of the apparatus. The temperature of the suspension was thermostatically controlled to within 0.1° C. of the desired value. Several alterations were made on the viscometer, a schematic drawing of which is shown in Figure 2. First, the liquid chamber and orifice of the commercial apparatus were replaced with another chamber and a capillary tube. The

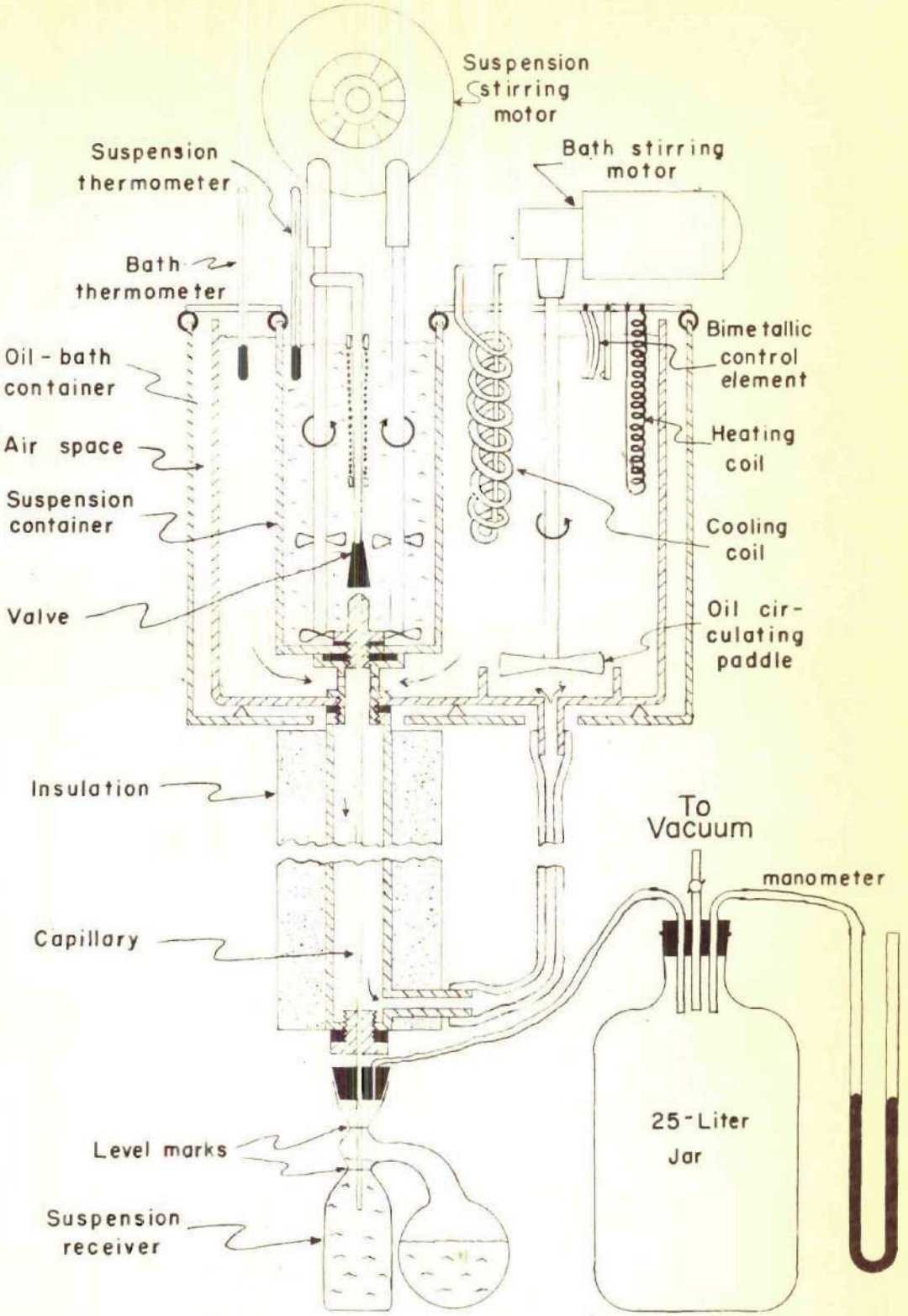

Figure 2. Suspension Viscometer.

flow-controlling valve was built inside of the fluid chamber, sealing the flow from above the capillary. This prevented it from plugging with sediment. Second, the thermostated section was extended to cover most of the length of the capillary tube by surrounding it with another tube through which thermostated oil was passed. Oil was forced through the tube by means of a propellor of greater pitch than was originally used. Third, the suspension was agitated by means of two multipaddle stirrers rotated in opposite directions by means of a Vari-Speed stirrer, distributed by Will Corporation, Rochester, New York. The orifice was located in relation to the stirrers so that relatively quiescent suspension entered the capillary. It is believed that this decreased the so-called end effect, yet provided for an ideal suspension. Fourth, a special suspension receiving bulb was designed to provide a nearly constant pressure against which flow occurred during any one run and to decrease the end effect at the lower end.

The receiving bulb was really two bulbs, with the capillary extending into the smaller one. Flow through the capillary was not timed, when making a run, until the smaller bulb had filled to the lower level mark. The run ended when the fluid filled the larger bulb and the level rose to the upper mark. Therefore, the liquid level remained almost constant through nearly all of the run. A volume of 53.58 ml. was contained between the level marks of the receiving bulb. Finally, a manometer, a 25-liter jar and an evacuating pump were arranged so that they could be attached to the receiving bulb and additional pressure drop could be applied across the capillary.

Two capillary tubes were used in the investigation. One had an

average internal diameter of 1.047 mm. and a length of 64.2 cm. and the other a diameter of 1.339 mm. and a length of 64.4 cm. As may be seen from Figure 2, the lower end of the capillary tube extended into the fluid container so that the vertical distance between the levels in the two containers was 67.8 cm. when a determination was started and was 66.2 cm. when the determination was completed. The fluid container of the viscometer was found to contain 304 ml. of fluid when filled to the level from which measurements were begun with the stirrer and thermometer in place. The chamber was 2-5/8 inches in diameter.

Auxiliary Equipment.--A glass pycnometer with a ground glass neck fitted with a thermometer reading directly to 0.2° C. was used to measure the densities of the solids, liquids and suspensions when necessary. The pycnometer, made by Kimble Glass Division of Owens-Illinois Glass Company, Toledo, Ohio, had a volume of approximately 25 ml.

Two different optical microscopes were used to determine the particle size of the materials used in this investigation. A laboratory type microscope with magnifications up to 970 diameters was used for the coarser particles. For the more finely divided materials, a research metallographic microscope which was capable of magnifications up to 1480 diameters was used. A filar micrometer eyepiece was used with both microscopes. All optical equipment was manufactured by the Bausch and Lomb Optical Company, Rochester, New York.

CHAPTER III

PROCEDURE

Viscosity Measurements.--When the viscosity of a liquid or suspension was to be determined, the viscometer chamber was filled to a fixed level with the fluid under investigation. The entire system was allowed to come to temperature equilibrium while being stirred at a low rate. The maximum stirring rate possible with the stirrer was used while all measurements were being made. When the seal on the capillary was released, liquid or suspension flowed through the capillary into the receiving bulb. A stopwatch was used to determine the time required for the liquid level to advance from the lower level mark on the receiving bulb to the upper level mark. The seal on the capillary was then replaced and a few minutes were allowed for large particles in the capillary to settle into the receiving bulb. The bulb was then removed and immediately replaced with a beaker of water or ethylene glycol, depending on the liquid in the viscometer at that time. It was found that if this were not done, the fine particles settling from the suspension remaining in the capillary would collect at the lower end and were difficult to remove without damage to the capillary.

If additional determinations were required at the same or at different flow rates, the fluid was returned to the apparatus and the procedure was repeated with the desired conditions. Different flow rates were obtained by increasing or decreasing the pressure in the

large jar connected to the receiving bulb. The effective head which produced the flow through the capillary was equal to the head of liquid or suspension plus the head change caused by the increase or decrease in pressure in the large jar. The pressure at the lower end of the capillary tube was practically unchanged during most of a run because of the design of the receiving bulb and because of the large volume connected to it and was considered constant. The pressure on the receiving flask was adjusted so that streamline flow was expected in most of the runs.

Calibration.--An identical procedure was used for calibrating the viscometer with the exception that fluids of known viscosities were used instead of the solid-liquid suspensions used above. One series of measurements was made for water with increased or decreased pressure drop produced by decreasing or increasing the pressure within the jar.

Preparation of Solutions and Suspensions.--The liquid-solid suspensions to be tested and the liquid solutions used for calibrating the viscometer were generally compounded in the desired concentrations by mixing weighed amounts of each component. Suspension samples taken in the course of a related heat transfer investigation were used in some cases. A wetting agent was necessary in order to disperse the solid material in the cases of graphite and aluminum powders mixed with water. Not more than 0.02 per cent by weight of the commercial wetting agent Aerosol O. T. of Stansi Scientific Supplies, Chicago, Illinois, was used for this purpose. The densities of the solid components and of each fluid system were obtained, either by direct measurement in a pycnometer or by calculation from the weights and densities of the

component materials.

Measurement of Settled Volume.--The volume occupied by the solid component in a bed formed by gravity sedimentation from the suspension was determined for each liquid-solid system investigated. This information was obtained by mixing a weighed quantity of the solid material with the liquid to be used in a graduated cylinder and allowing the suspension to settle for a long time under the influence of gravity. The volume occupied by the sedimented bed was then read directly on the cylinder. Some of the suspensions stood for more than a month; however, no change was observed in any case after a few days. The same wetting agent was employed and in the same proportions for graphite and aluminum powder in water as was used in the investigations for viscous properties.

Measurement of Size Distribution.--The size distribution of each of the solid materials used in this investigation was determined by measuring the diameter of a large number of particles in the optical microscopes described above. Approximately 150 particles were measured for each material. The data were then analyzed graphically as described by DallaValle (1948) to get the size distributions for each material.

Recording of Data.--The data taken during the viscosity measurements for each fluid system employed were (1) the volume per cent of solids in the fluid system (or weight per cent of glycerine in the case of the liquid solutions), (2) diameter of the capillary tube, (3) temperature of the fluid system, (4) density of the fluid system, (5) time of efflux of 53.58 ml. of fluid from the capillary and (6) vacuum or pressure applied to the receiving flask. These data are presented in Table

1 in the Appendix. In addition, (1) the density of the particles used, (2) the median size of the particles, (3) the geometric standard deviation of the particles and (4) the volume of solids in the settled bed, in each fluid system employed are recorded in Table 2 in the Appendix.

CHAPTER IV

ANALYSIS OF DATA

Calibration of Apparatus.--Since the level of the liquid or suspension in the viscometer decreased during a determination, the head or pressure causing the flow decreased. The effective head was found to be the logarithmic mean head and may be written

$$H = (H_1 - H_2)/\ln(H_1/H_2) , \qquad (9)$$

where H_1 is the head at the beginning of the measured time interval and H_2 is the head at the end of the measured time interval. The derivation of this equation and of Poiseuille's law, from which it is derived, is given in the Appendix. In five determinations of the head of fluid under gravity flow, the location of the receiving bulb was altered only slightly and the effect was negligible. The average value of H_1 was found to be 67.8 cm. and that of H_2 to be 66.2 cm., resulting in a value of 67.0 cm. for the logarithmic mean head of fluid under gravity flow as calculated from Equation 9. The pressure drop through the capillary was obtained by multiplying this value by the density of the fluid in the viscometer.

When decreased or increased pressure drop was produced by decreasing or increasing the pressure in the receiving bulb, this additional pressure was added to the logarithmic mean head which resulted from the column of fluid alone; these data were used in preparing shear

diagrams as discussed below.

The capillary viscometer is essentially a simple device in which a fixed volume of fluid flows through a capillary tube of certain length and diameter under the influence of a given pressure in a certain time. However, every instrument of the type used in this investigation has a certain inherent defect for which correction must be made if accurate results are to be obtained. The liquid undergoes an acceleration as it enters and when it leaves the capillary tube. Some turbulence is also introduced so that only a part of the work done by the driving force is accounted for by the friction within the capillary tube. A correction must be applied which is called the kinetic energy correction.

Poiseuille's equation, derived in the Appendix, may be written

$$\mu = \pi D^4 g_c t \Delta P / 128 L V \ , \qquad (10)$$

where D is the diameter of the capillary, ΔP is the pressure drop through the capillary, L is its length and V is the volume of fluid flowing through the capillary in the time t. It is based on the assumption that all energy is employed in overcoming the viscous resistance of the liquid and is strictly applicable only to conditions in a length of the capillary where neither turbulence nor acceleration are present. An early attempt to arrive at the kinetic energy correction was made by Hagenbach (1860), but Wilberforce (1891) detected a slip in Hagenbach's reasoning and is generally given credit for arriving at the correct relationship. However, Bingham (1922) states that others had arrived at the same result previously. The corrected relationship may

be written

$$\mu = \frac{\pi D^4 g_c t \Delta P}{128\ LV} - \frac{m\rho V}{8\pi L t} \quad , \tag{11}$$

where m is a constant that depends on the design of the viscometer. When streamline flow exists throughout the length of the capillary tube, Hall and Fuoss (1951) contend that m = 1, but that in fact, turbulence is introduced at each end of the capillary tube and the value of m is unknown. However, because much experimental evidence indicates that Equation 11 should be accepted, they recommend that the actual analysis be made graphically using the form of this equation. For an instrument of the type used in this analysis, with a fixed head of flow and with identical volumes of fluid flowing in each run, this equation can be put in the form

$$\mu/\rho = at - b/t \quad , \tag{12}$$

where

$$a = \pi D^4 g_c \Delta P / 128 LV\rho$$

and

$$b = mV/8\pi L \quad .$$

Since the pressure drop through the capillary is caused by the head of fluid, ΔP is directly proportional to ρ and $\underline{a}$ is a constant, even though it contains ΔP and ρ, both variables. Multiplying both sides of Equation 12 by t and noting that $\mu/\rho = \nu$, the kinematic viscosity, a linear form of the equation,

$$\nu t = at^2 - b \quad , \tag{13}$$

is obtained. The constants a and b may be evaluated as the slope and intercept, respectively, of the straight line resulting when νt is plotted as ordinate versus t^2 as the abscissa. The viscometer was calibrated by this procedure using the data from the water and water-glycerine measurements with the two capillary tubes. A recent determination of the viscosity of water at 20° C. with greater accuracy than was formerly possible was reported in Chemical and Engineering News (1952). The new value, 0.01002 poise, indicates that the values given by Lange (1949) are about 0.3 per cent too high. However, the viscosities and densities of these liquids as given by Lange were accepted as correct, since the resulting error is less than the other experimental errors involved in these measurements. The viscosity and density of the ethylene glycol were taken from a publication of the Carbide and Carbon Chemicals Corporation (1947). The calibration curves are shown in Figure 3. The points plotted in this figure and the resulting values for the constants a and b of Equation 12 are given in Table 3 in the Appendix.

Calculation of Viscosities.--The viscosities of the suspensions were calculated from the experimental data taken when the suspensions flowed under a pressure equivalent to their head only, using Equation 12 and the values of a and b obtained by the calibration. As an example, Run No. 27 was made with the 1.339 mm. capillary under gravity flow (See Table 1.). In this run, a suspension of water and 16.00 volume per cent graphite at a temperature of 36.0° C. had a density of 1.154 g./ml. and required 13.497 minutes to fill the viscometer receiving bulb. From Table 3 the constants a and b are seen to be 0.9800 and 0.092,

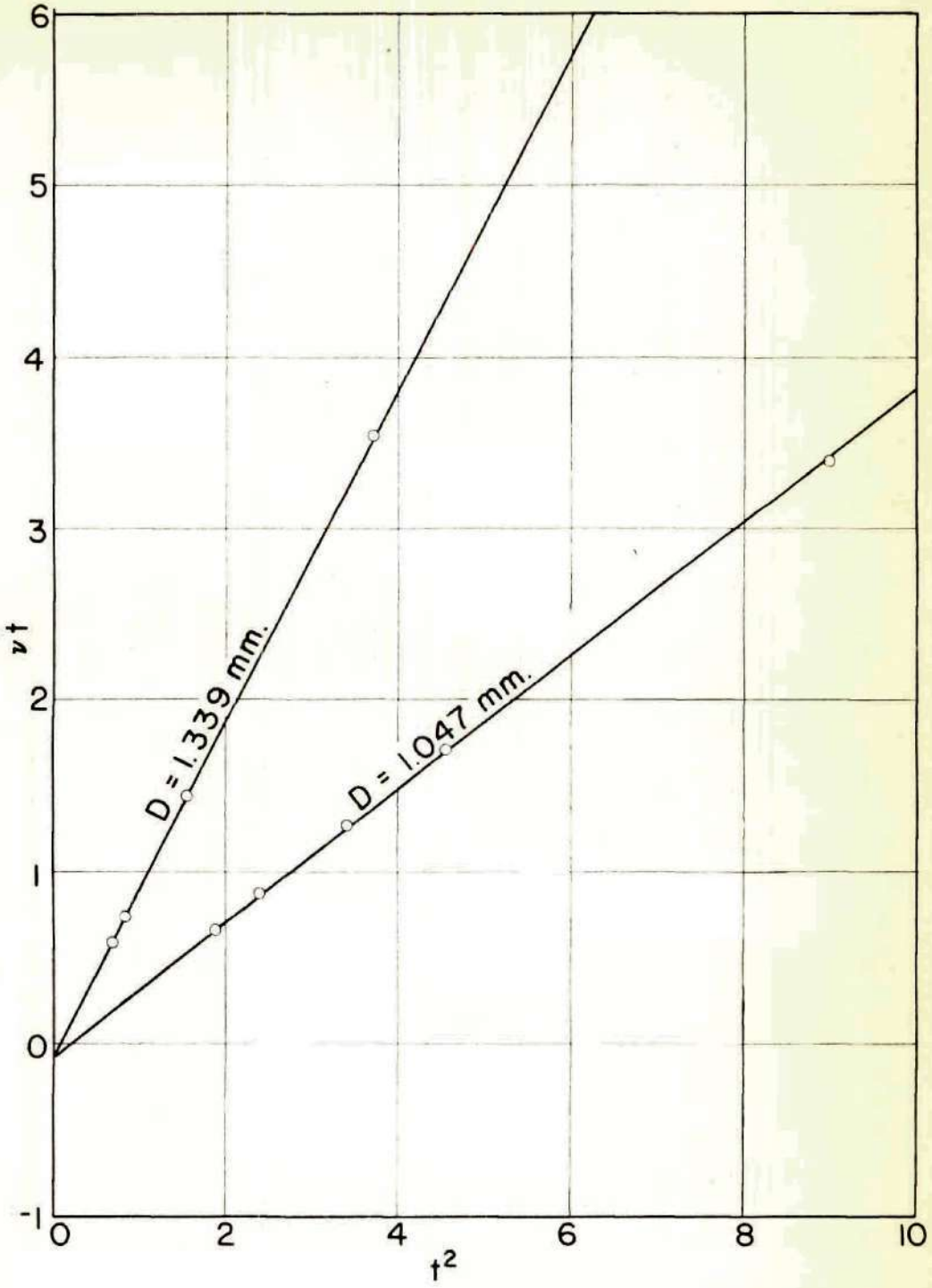

Figure 3. Calibration Curves for the Two Capillaries Used with the Viscometer.

respectively, when time is expressed in minutes, viscosity in centipoise and density in grams per milliliter. Then, using Equation 12,

$$\mu = a\rho t - b\rho/t = 0.9800 \times 1.154 \times 13.497$$
$$- 0.092 \times 1.154/13.497 = 15.54 \text{ centipoise.}$$

This value of the viscosity is shown for Run No. 27 in Table 4 in the Appendix.

In order that results from different suspensions might be more readily compared, the concentration of solids in the suspension and the resulting viscosities were computed on a reduced basis. Thus, the reduced volume of solids is defined as the ratio of the volume fraction of particles in the suspension, C, to that in a settled bed, C_s. The reduced viscosity is similarly defined as the ratio of the viscosity of the pure liquid phase, μ_o, to that of the suspension, μ, at the same temperature. Thus for the example above, C_s may be found from Table 2 to be 0.264 and then $C/C_s = 0.606$. The viscosity of water at 36.0° C. is given by Lange (1949) as 0.707 centipoise and from the viscosity of the suspension calculated above, μ is seen to be 15.54 centipoise and $\mu_o/\mu = 0.064$. Values of C/C_s and μ_o/μ were calculated for each run by gravity flow and are also presented in Table 4 in the Appendix.

Calculation of Shear Diagrams.--Flow measurements were made at different rates of flow on three of the fluid systems in order that shear diagrams might be obtained. The shear diagrams give a better indication of the viscous behavior of the suspensions, although the analysis is not strictly correct. One source of error is due to the fact that the kinetic energy correction discussed above is neglected. This

introduces an error of several per cent in the case of water, however, the error is negligible for the more viscous suspensions. A second inaccuracy is due to the fact that a relationship which holds for Newtonian fluids only is applied to non-Newtonian fluids. However, the analysis is widely used for classifying fluids (See for example, Alves (1949)).

Equation 10 can be put in the form

$$\mu = \frac{D^2 g_c \Delta P}{32 L v} = \frac{g_c D}{8v} \cdot \frac{D\Delta P}{4L} \quad , \tag{13}$$

where v is the velocity of flow. The reciprocal of the first factor on the right is the rate of shear at the capillary wall and the second factor is the shear stress at the same point. When $8v/g_cD$ is plotted as ordinate and $D\Delta P/4L$ as abscissa, the viscosity, or apparent viscosity, is given by the inverse slope of the line through the origin and the particular point in question. The Reynolds numbers that prevailed during the experimental runs may also be calculated if the viscosity of the suspension is known. Three shear diagrams, showing three lines of constant Reynolds number are given in Figures 4, 5 and 6.

A suspension of the same concentration and of identical materials but at a different flow rate will be used to illustrate the calculation of the shear diagrams. In Run No. 28, all of the conditions of Run No. 27 were duplicated except that a vacuum of 11.43 millimeters of mercury was applied to the flask and the time of efflux was only 2.030 minutes. Since 53.58 milliliters of suspension flowed through the capillary in the time interval, the rate of shear at the capillary wall

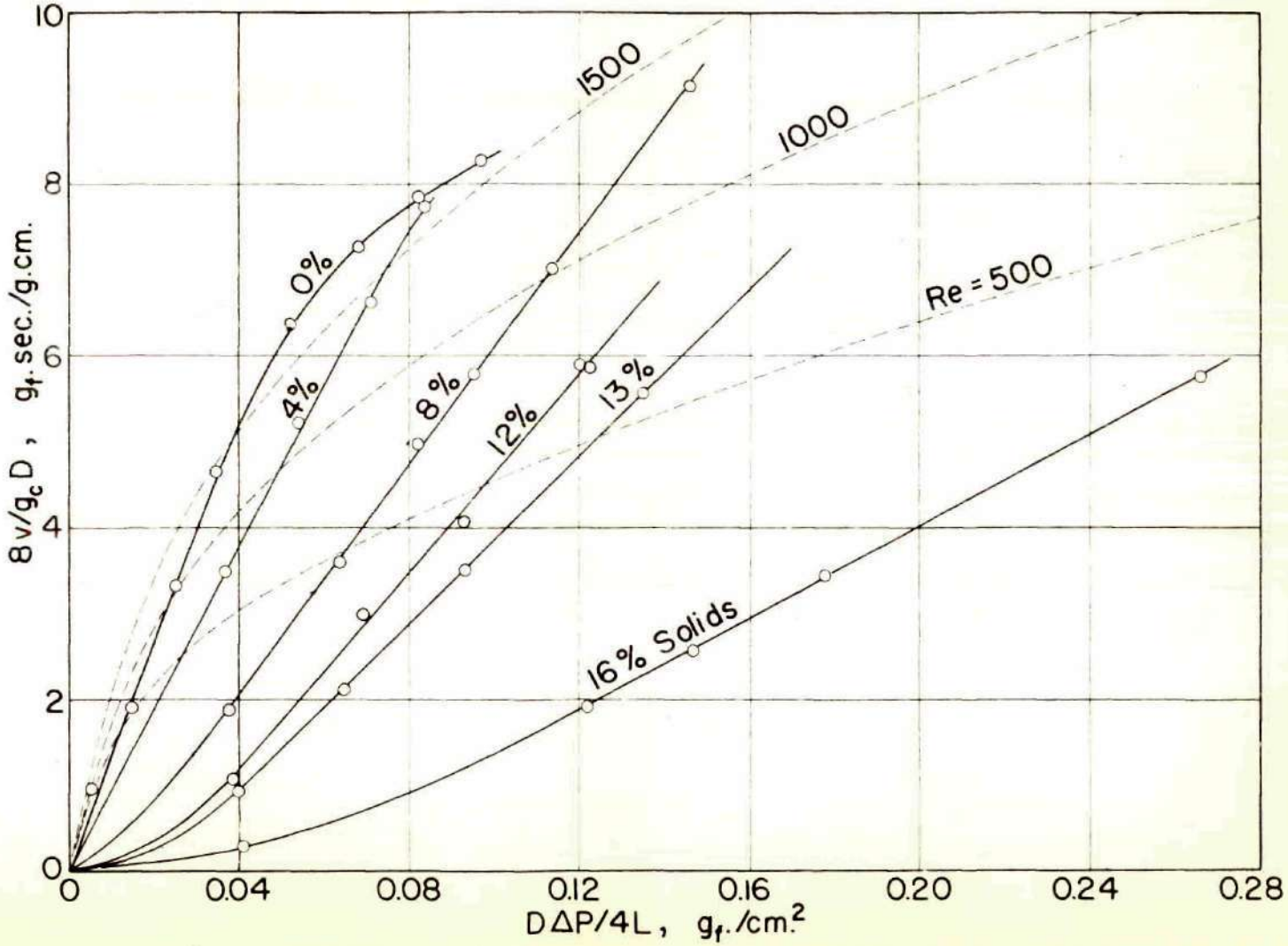

Figure 4. Shear Diagrams of Water-Graphite Suspensions Showing Lines of Constant Reynolds Number.

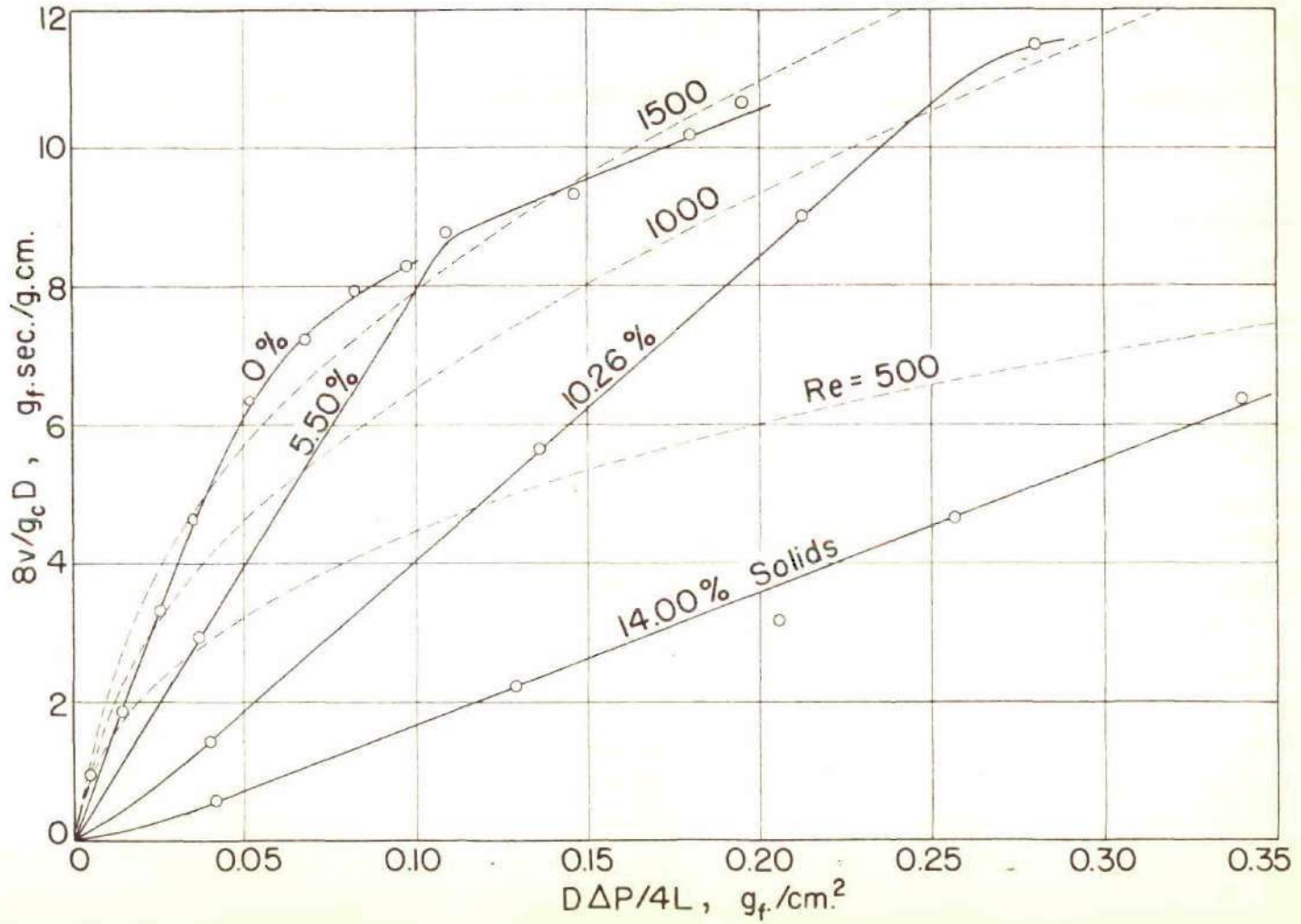

Figure 5. Shear Diagrams of Water-Attaclay Suspensions Showing Lines of Constant Reynolds Number.

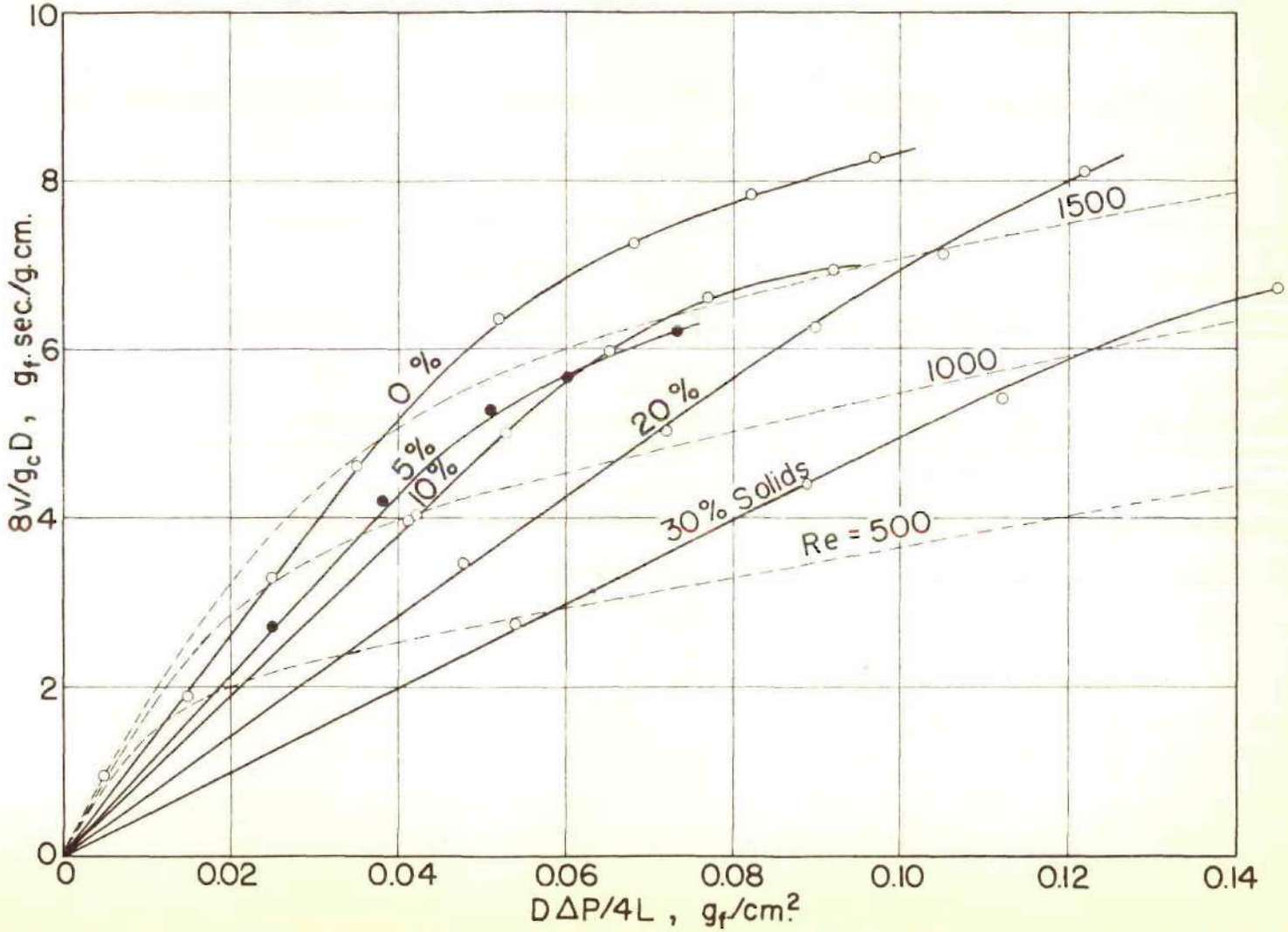

Figure 6. Shear Diagrams of Water-No. 18 Glass Suspensions Showing Lines of Constant Reynolds Number.

was calculated to be

$$\frac{8v}{g_c D} = \frac{8 \times (53.58/60 \times 2.030)}{981 \times 0.1339} = 1.91 \ g_f.\text{sec.}/g.\text{cm.}$$

The pressure drop through the capillary is equal to that due to the head of liquid in the viscometer plus that due to the vacuum applied to the flask and indicated by the mercury manometer. Then for Run No. 28

$$\Delta P = (\rho H)_{\text{capillary}} + (\rho H)_{\text{manometer}}$$
$$= 1.154 \times 67.0 + 13.55 \times 11.43 = 234 \ g_f./\text{cm}^2.$$

The shear stress may then be calculated directly as

$$\frac{D\Delta P}{4L} = \frac{0.1339 \times 234}{4 \times 64.4} = 0.122 \ g_f./\text{cm}^2.$$

Values of the pressure drop, shear stress and rate of shear are given in Table 5 in the Appendix.

Lines of constant Reynolds number were obtained by using Reynolds number in the form

$$Re = vD\rho/\mu_a \ ,$$

where μ_a is the apparent viscosity, and solving for **v**. This value of v was then substituted into the expression for the rate of shear. The value of the apparent viscosity was obtained as the inverse slope of a point on one of the shear diagrams. As an example, consider the shear diagram of the water-graphite suspension containing 8 volume per cent solids obtained with the 1.339 mm. capillary shown in Figure 4. By

assuming a rate of shear of 10.00 g_f.sec./g.cm., at a Reynolds number of 1500, the apparent viscosity was found to be 1.580 centipoise (or 0.01580 g./cm.sec.). The density of this suspension at 36.0° C. was 1.073 g./ml. The rate of shear was then calculated to be

$$\frac{8v}{g_c D} = \frac{8Re\mu_a}{g_c D^2 \rho} = \frac{8 \times 1500 \times 0.01580}{981 \times (0.1339)^2 \times 1.073} = 10.04 \frac{g_f.sec.}{g.cm.} .$$

This value of the rate of shear is in good agreement with the assumed value and is shown in Table 6. Since the apparent viscosity of non-Newtonian suspensions is not constant, the assumed value of shear stress may not coincide with the calculated value. However, a second calculation, based on the previously calculated value usually gave a good check. Calculated values of the apparent viscosity and rate of shear calculated for Reynolds numbers of 1500, 1000 and 500 are given in Table 6 for the shear diagrams in Figures 4, 5 and 6.

Correlation of Results.--It has been noted by Bingham and Durham (1911) that the fluidity of a dilute suspension (proportional to μ_o/μ) decreases essentially linearly with an increase in concentration (proportional to C/C_s) so that, if this linear portion were extrapolated, a fluidity of zero would be indicated at a rather low concentration. Bingham and Durham have also shown that the concentration at which the fluidity would be zero appears to be independent of the temperature. As the concentration increases, however, the linear relation fails and a fluidity of zero is indicated at a considerably higher concentration of the solid material. This higher concentration of zero fluidity also appears to be independent of temperature. Orr (1952) has shown that a

given concentration of solid material changes the viscosity of the suspension the same relative amount regardless of temperature. Reiner (1949) states that the change in the viscosity of a suspension with temperature is entirely due to the viscosity of the liquid. This is in agreement with the above observation.

A fluidity of zero, which means an infinite viscosity, cannot occur unless each particle is in contact on all sides with other particles, in other words, unless it is in a bed. Measured viscosity-concentration data permit considerable leeway in locating the point of zero fluidity, but smooth curves were obtained in every case by Orr (1952) and by Orr and DallaValle (1954) when this point was taken as that representing conditions in a bed produced by gravity settling. On the basis of the above reasoning, Orr and DallaValle arrived at the empirical relationship cited in Chapter I which may be expressed as

$$\mu_o/\mu = (1 - C/C_s)^k \ , \qquad (14)$$

where the constant k is equal to 1.8. They found that, while not entirely satisfactory, this equation gave better agreement with experimental results than did any of the other relationships given in Chapter I with the possible exception of Equation 4, which required three unknown constants and was not checked.

The value of the constant in Equation 14 may be evaluated easily by plotting μ_o/μ versus $(1 - C/C_s)$ on log-log paper, providing a straight line is obtained. This is indeed the case, as is shown in Figures 7, 8 and 9. The slope of this line is equal to the constant k in Equation 14. Values of μ_o/μ and of $1 - C/C_s$ for all suspensions

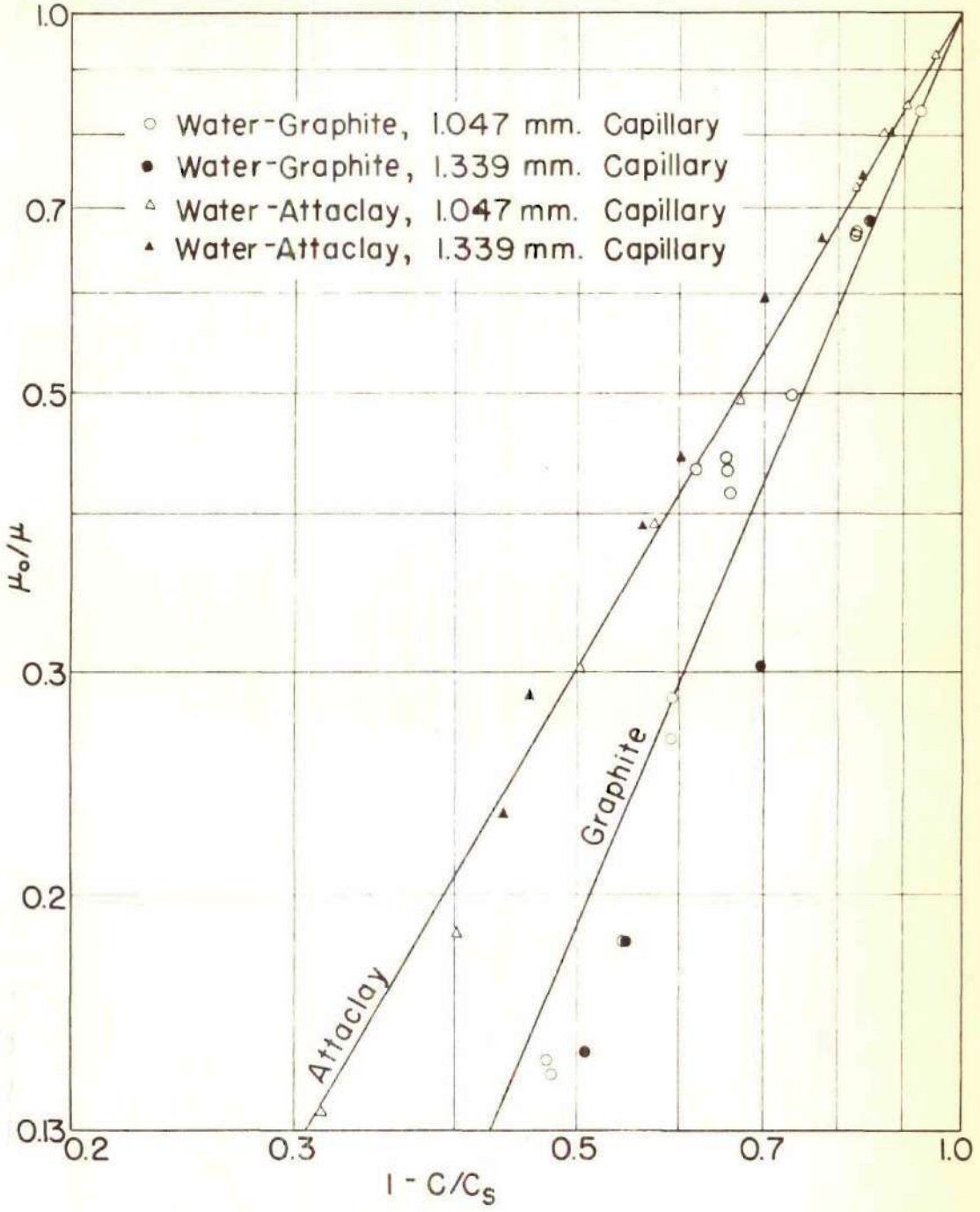

Figure 7. Plot of Equation 14 for Suspensions of Water with Graphite and with Attaclay Using Two Different Capillaries.

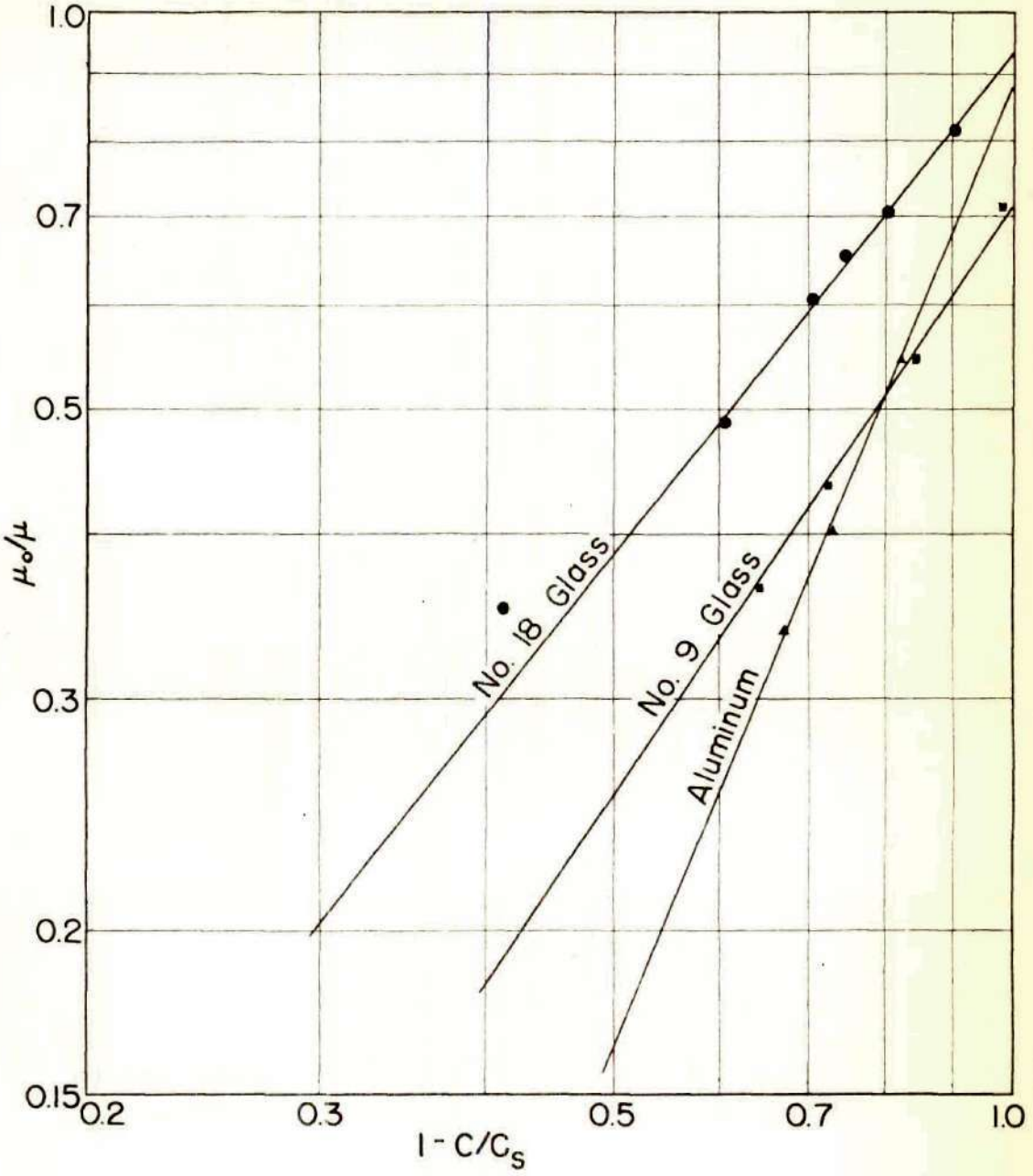

Figure 8. Plot of Equation 14 for Suspensions of Water with No. 18 Glass, with No. 9 Glass and with Aluminum Using the 1.339 mm. Capillary.

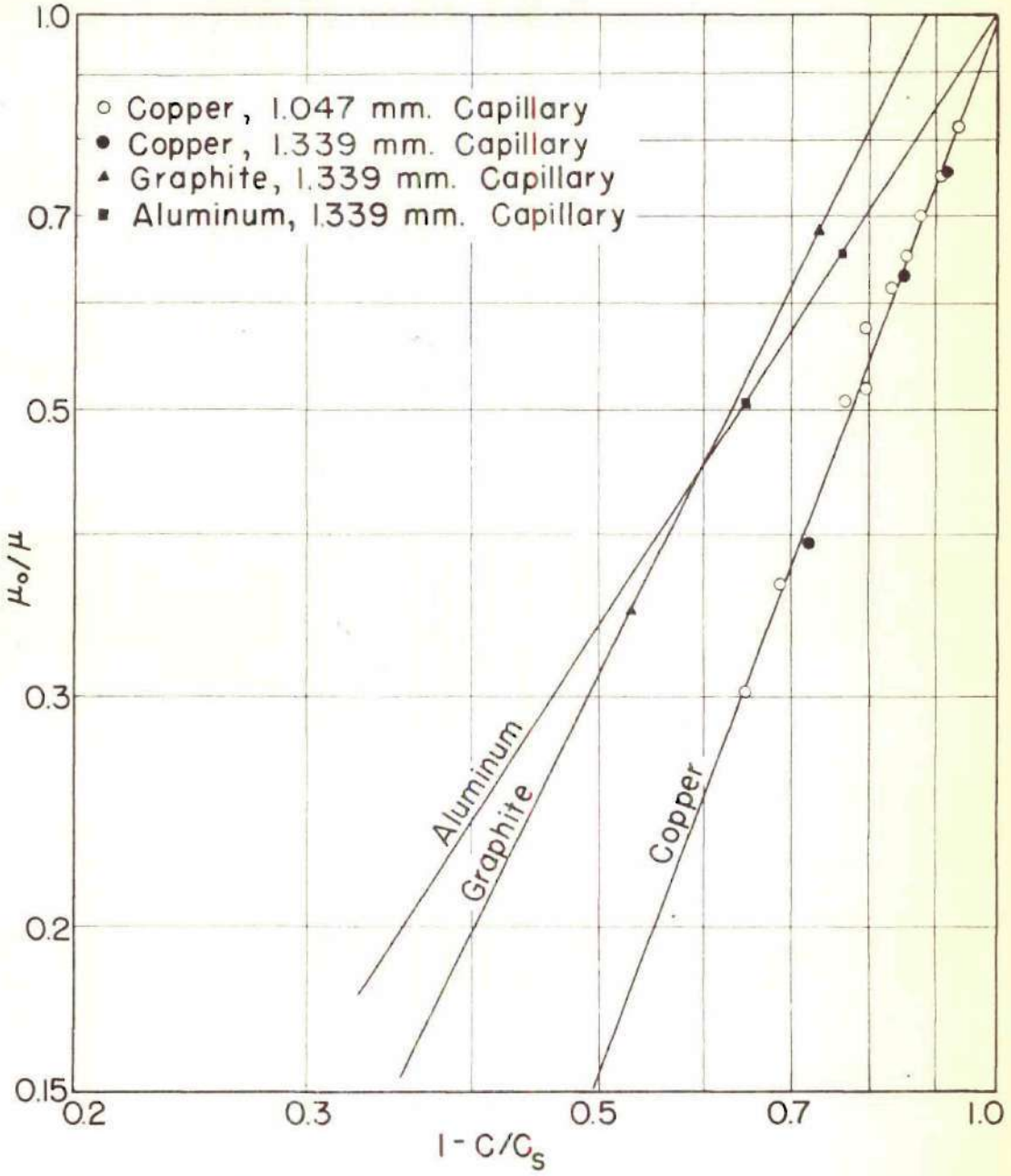

Figure 9. Plot of Equation 14 for Suspensions of Water with Copper and of Ethylene Glycol with Graphite and with Aluminum.

measured under gravity flow are given in Table 4 in the Appendix. Values of the constant k, calculated from the lines in Figures 7, 8 and 9, are recorded in Table 2 in the Appendix.

An examination of the values of k and of the geometric standard deviation, σ, in Table 2 in the Appendix indicated that they were approximately equal. The correlation of these two characteristics is more obvious in Figure 10, where k is plotted versus σ on an arithmetic grid and on a logarithmic grid. In both cases, a straight line with a slope of 45° gives a reasonably good fit. It has therefore been assumed that the value of the constant k in Equation 14 is equal to the geometric standard deviation of the suspended material. The curves in Figures 11 through 14 were calculated from Equation 14 and from the equation

$$\mu_o/\mu = (1 - C/C_s)^{\sigma} \quad . \tag{15}$$

The geometric standard deviation was determined graphically from the size distributions of the suspended materials shown in Figure 15. As shown by DallaValle (1948),

$$\sigma = \frac{84.13 \text{ per cent size}}{50 \text{ per cent size}} = \frac{50 \text{ per cent size}}{15.87 \text{ per cent size}} \quad . \tag{16}$$

For example, the geometric standard deviation of the graphite is

$$\sigma = 9.97/4.41 = 4.41/1.95 = 2.26 \quad .$$

A cursory examination of factors affecting the viscosities of suspensions might indicate that particle size and shape should also be

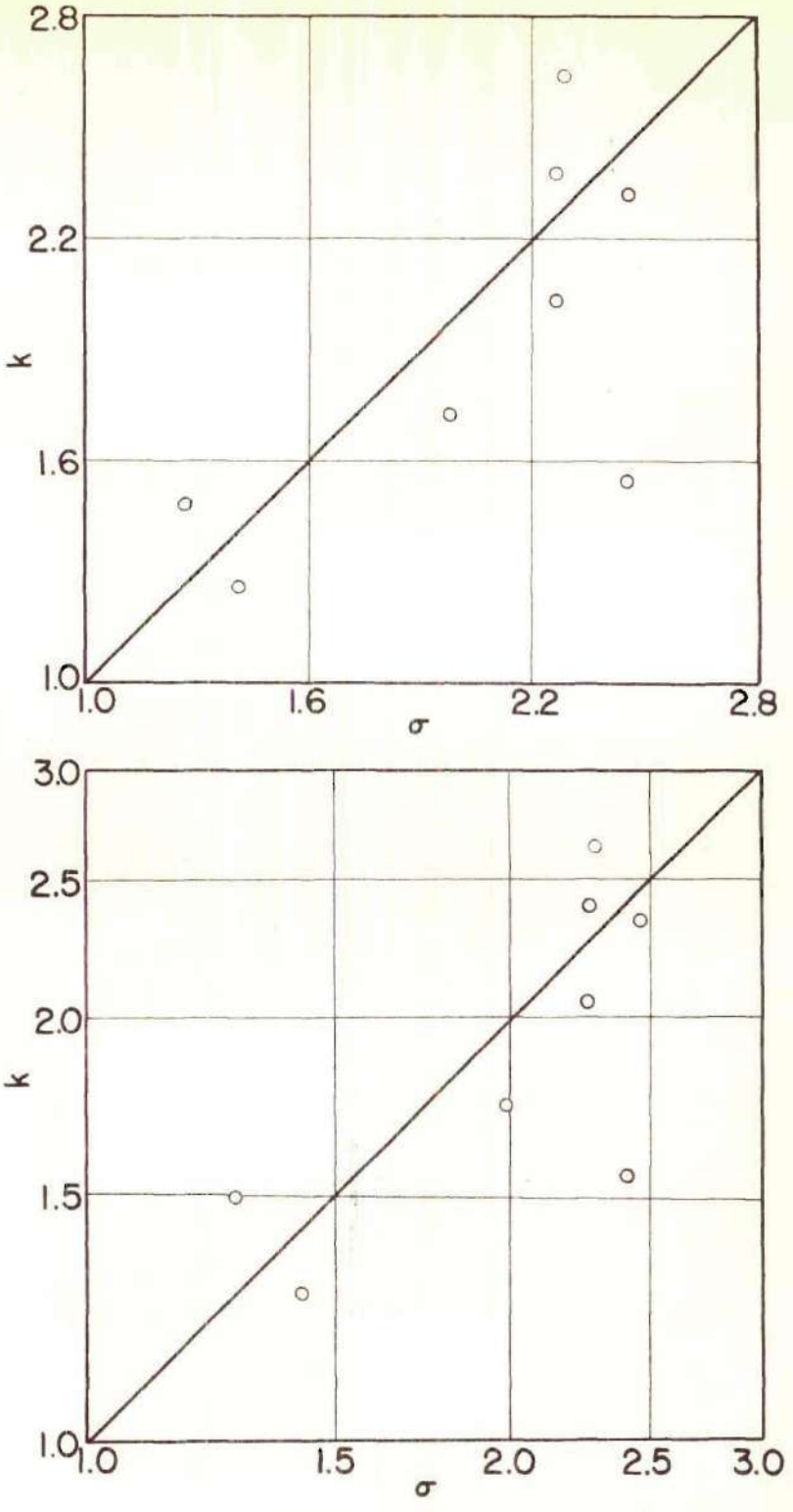

Figure 10. Arithmetic and Logarithmic Plots of k in Equation 14 versus the Standard Deviation of the Suspended Materials.

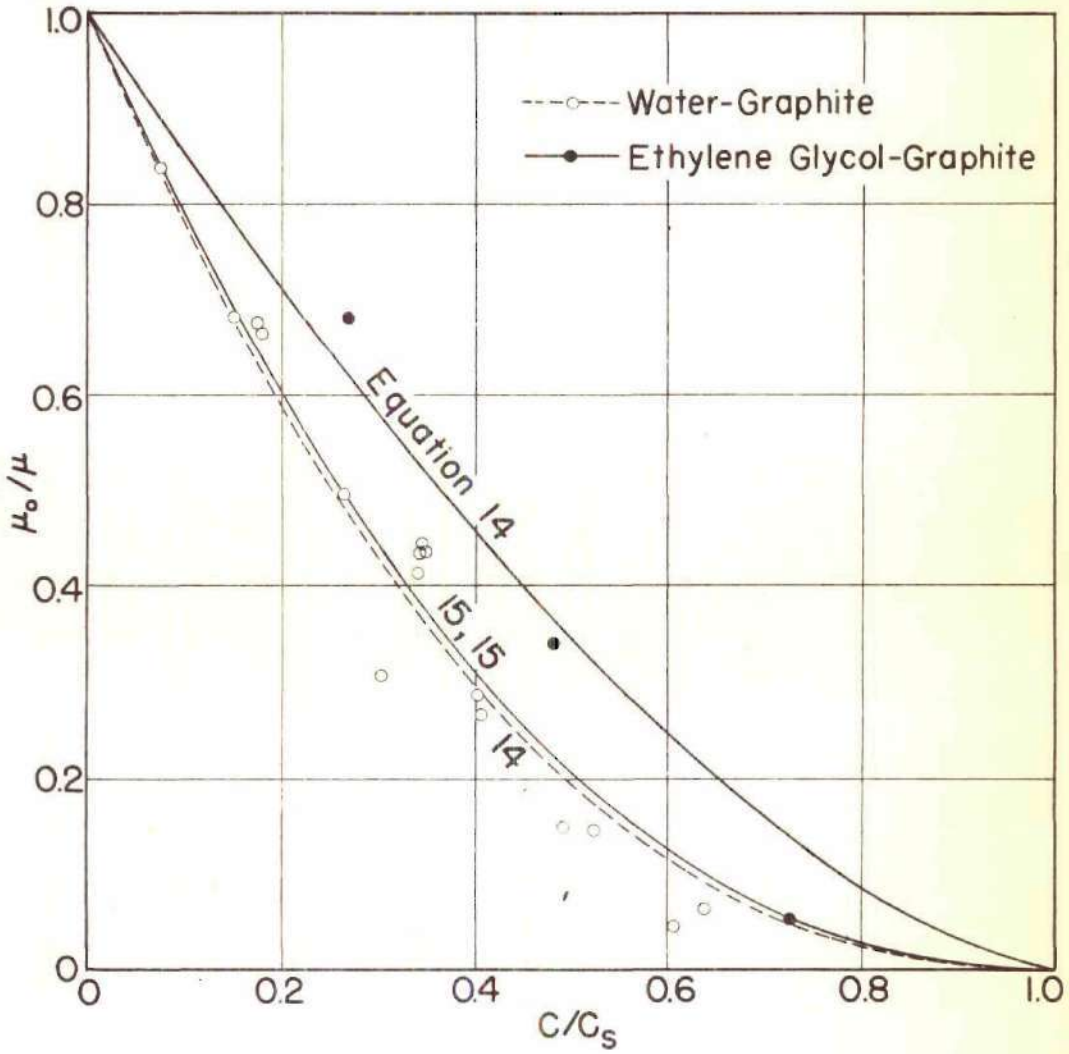

Figure 11. Reduced Viscosities of Suspensions of Graphite in Water and Ethylene Glycol. The Points are Experimental Values and the Lines are Plots of Equations 14 and 15.

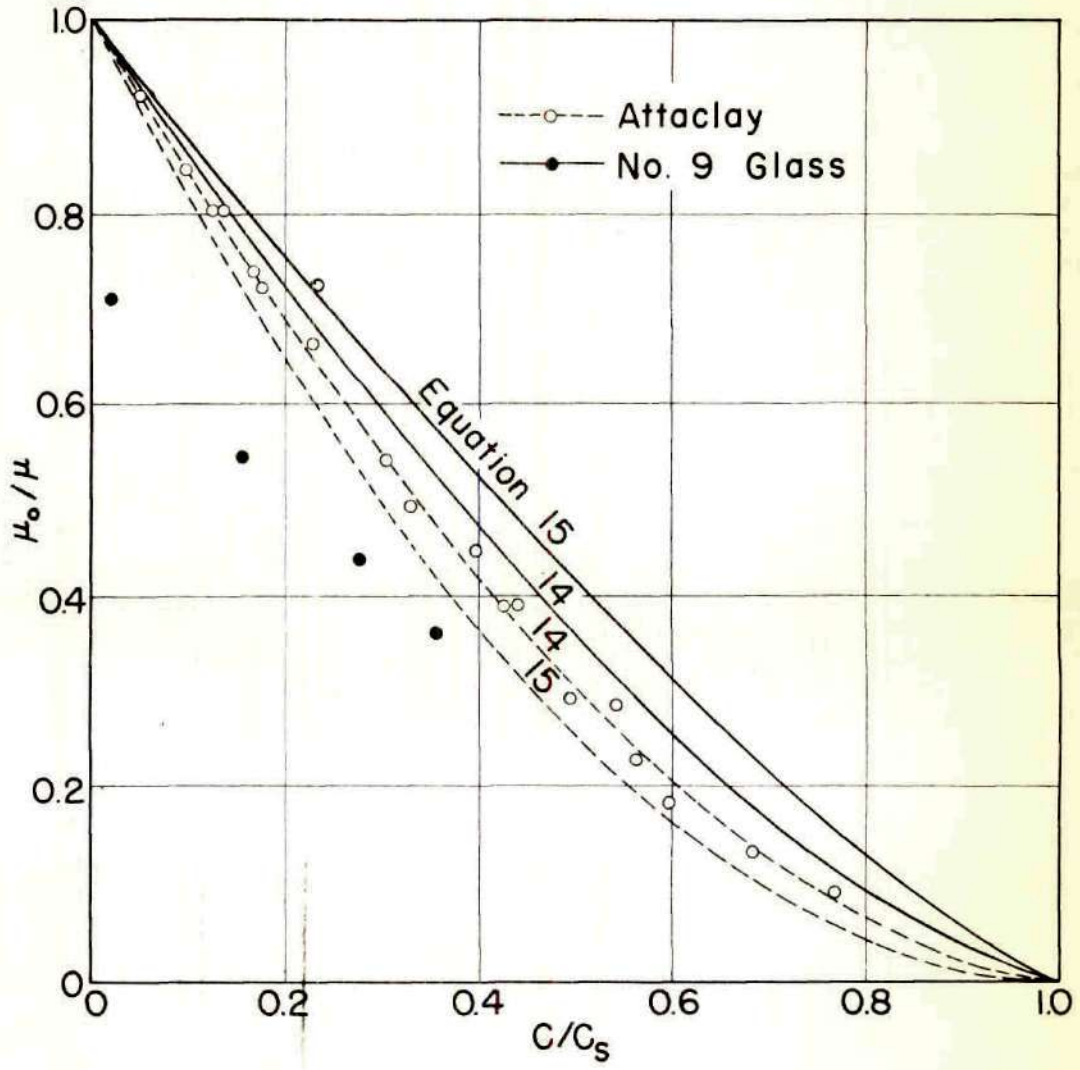

Figure 12. Reduced Viscosities of Suspensions of Attaclay and No. 9 Glass in Water. The Points are Experimental Values and the Lines are Plots of Equations 14 and 15.

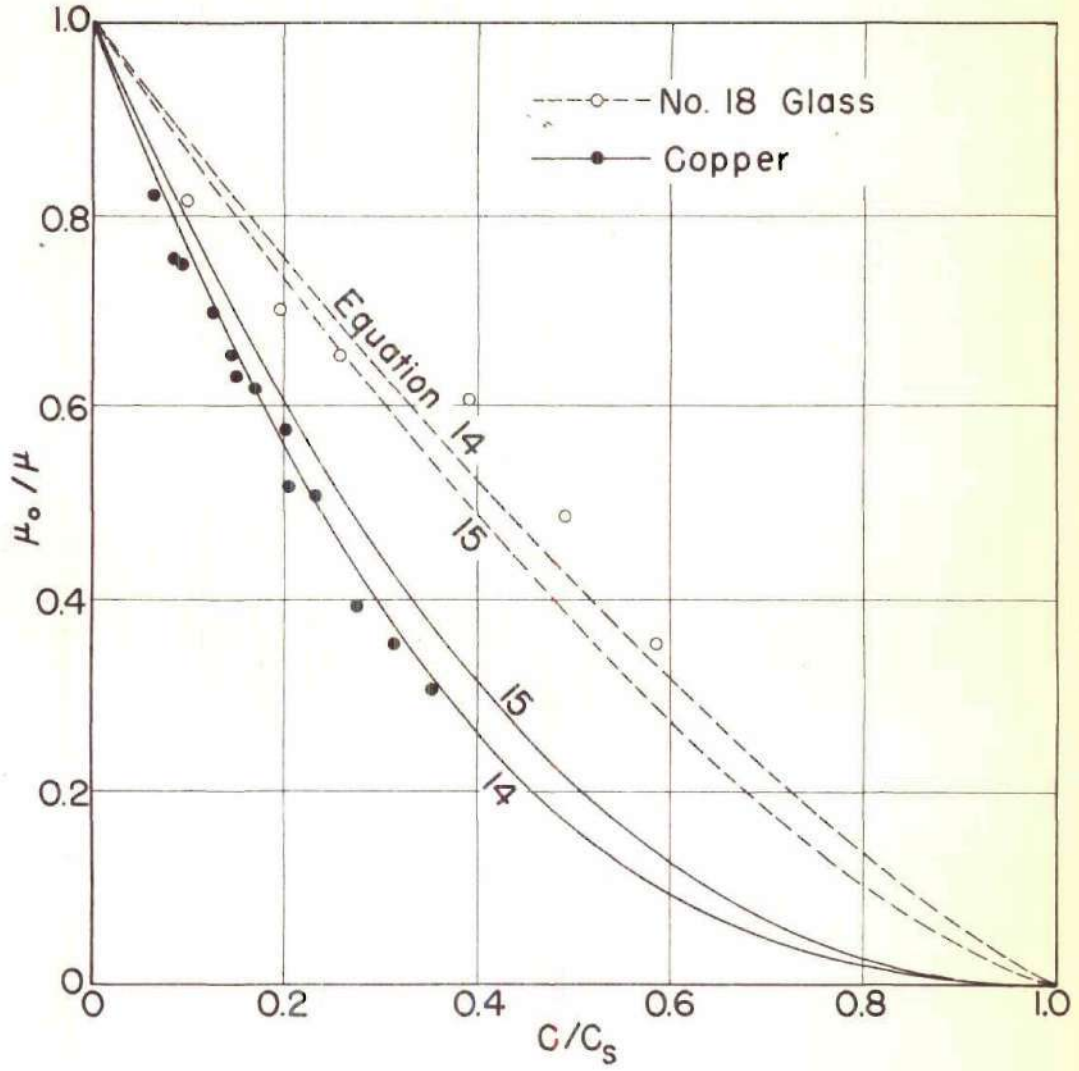

Figure 13. Reduced Viscosities of Suspensions of No. 18 Glass and Copper in Water. The Points are Experimental Values and the Lines are Plots of Equations 14 and 15.

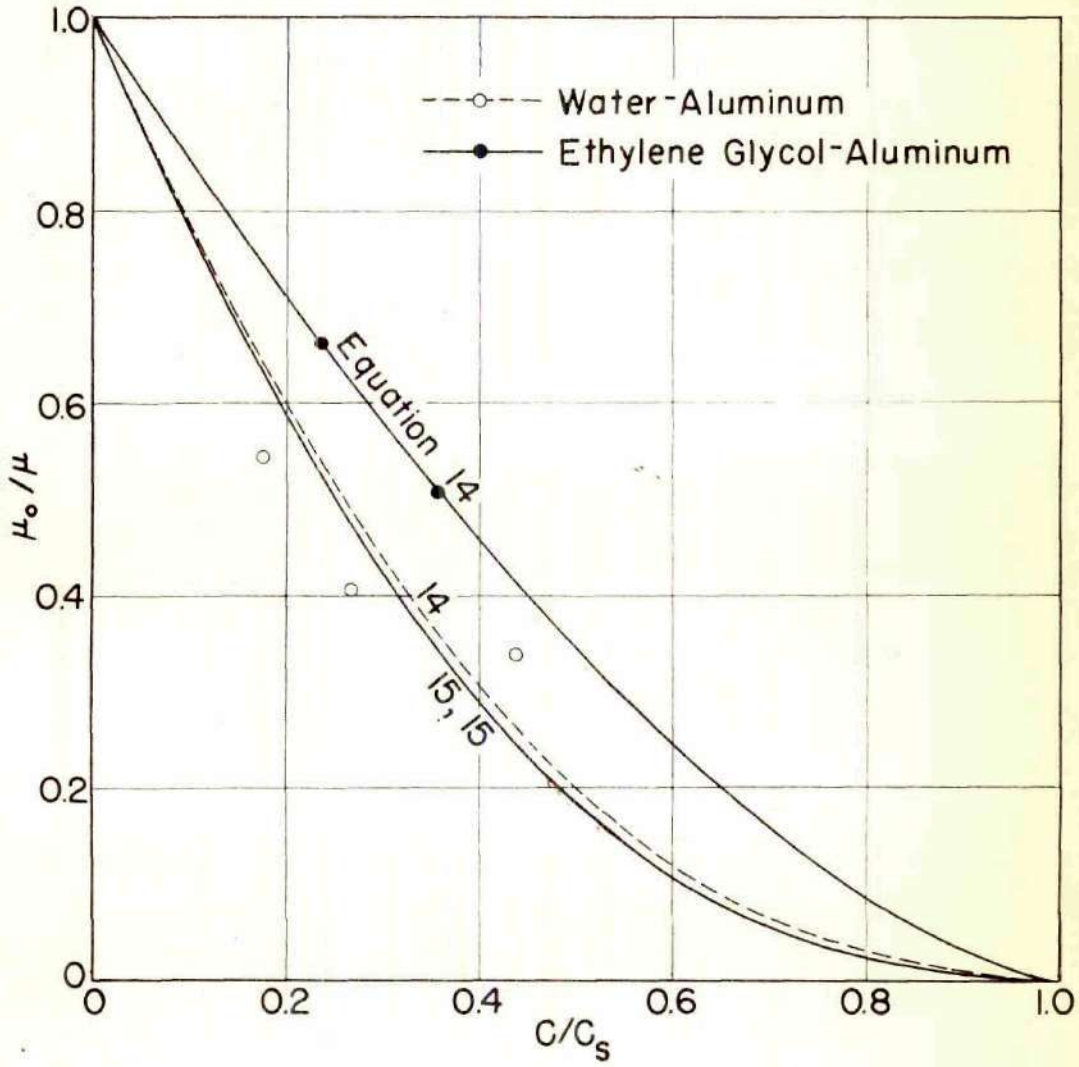

Figure 14. Reduced Viscosities of Suspensions of Aluminum in Water and Ethylene Glycol. The Points are Experimental Values and the Lines are Plots of Equations 14 and 15.

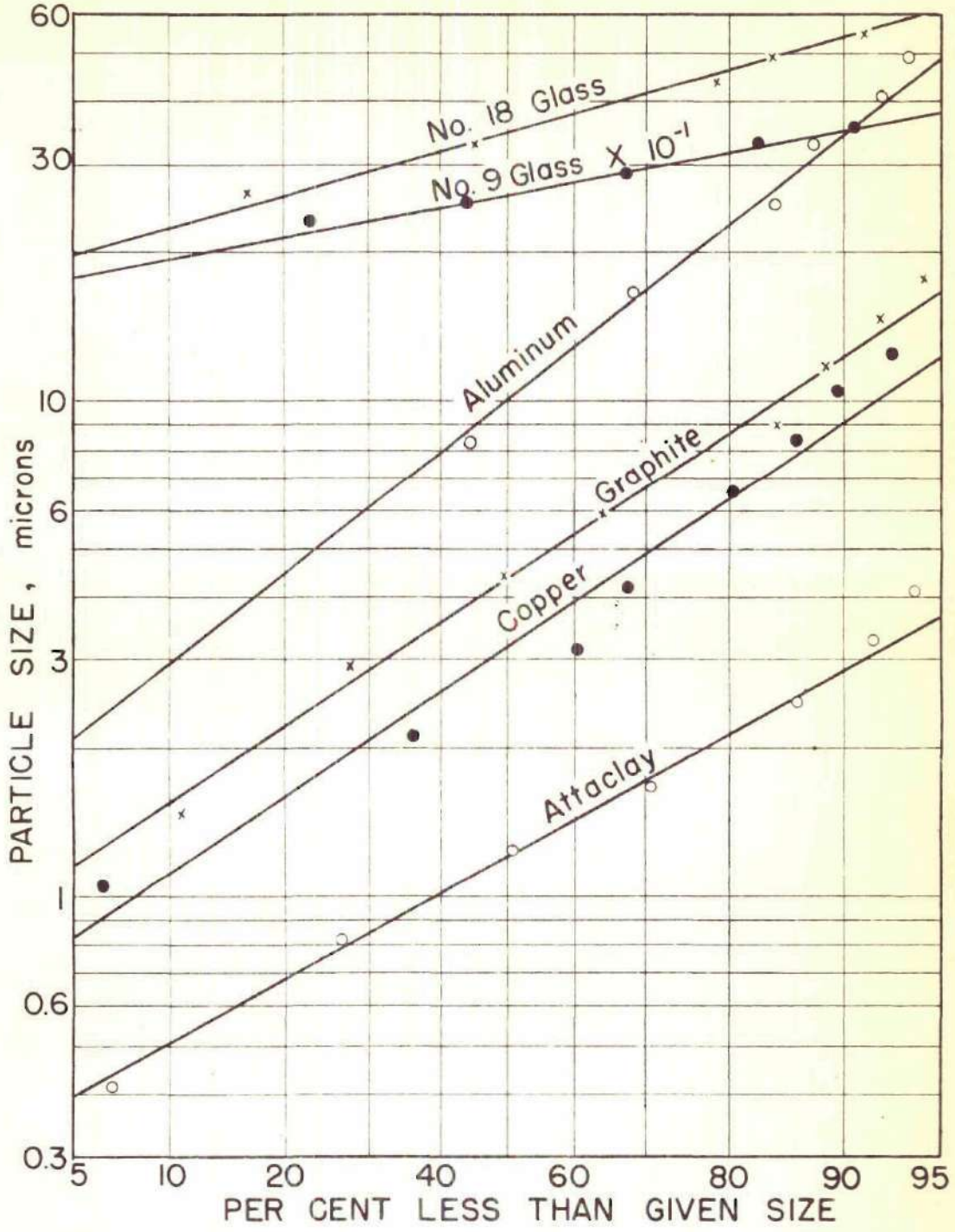

Figure 15. Particle Size Distribution of Solid Components of Fluid Systems.

considered. However, further examination will show that particle size need not be considered except in relation to capillary diameter and settling velocity as discussed in the following chapter. It may seem surprising that particle size itself should not have some effect on the viscosity of the suspension. However, as Reiner (1949) explains, the energy which a viscous material dissipates per unit volume is an indication of its viscosity, or of the resistance of the material to flow. If a rigid particle is present in the liquid, the additional energy dissipated per unit volume due to the particle cannot depend on the scale of the system. The volumes of both the particle and the liquid decrease as the third power of a linear reduction in scale, and the volume concentration is unchanged. However, the surface of the particle decreases as the second power and its length as the first power. Therefore, neither the surface of the particle nor its length, or size, can have any influence on the viscosity, if the scale has no influence. This reasoning is based on the assumptions that the shape of the particle is fixed and that the liquid is completely homogoneous, and fails if the shape of the particle changes or the size of the particle approaches that of the liquid molecules.

The shapes of the particles used varied from almost perfect spheres to flat plates and an attempt was made to evaluate the effect of particle shape. It was noted that the settling volume was larger for the more nearly spherical particles as well as for those with smaller geometric standard deviations. No direct correlation was found. However, the effect of particle shape and size distribution on viscosity are indirectly considered in the settled volume.

CHAPTER V

DISCUSSION OF RESULTS

Capillary Measurements.--As may be seen from Figure 3, the calibration data for the two capillary tubes used deviated very little from straight lines. These lines had identical intercepts but different slopes. Further examination revealed that the slopes of the lines are proportional to the fourth power of the capillary diameters. This fact is in accordance with Equation 12, since the constant a contains the diameter of the capillary raised to the fourth power. The constant b is independent of the diameter of the capillary and, therefore, should be the same for both capillaries.

Except for the higher concentrations, the shear diagrams in Figures 4, 5 and 6 indicate that most of the suspensions were essentially Newtonian fluids. Therefore, the viscosities indicated by the capillary viscometer should be accurate indications of the viscosities under all laminar conditions. This is not true for the more concentrated suspensions, which are non-Newtonian. The apparent viscosities of these suspensions change with an increase in the rate of shear, and the viscosities indicated in the viscometer are only the apparent viscosities at particular rates of shear. For these suspensions, a more detailed study is necessary to evaluate the flow properties.

Shear Diagrams.--The shear diagrams for three of the suspensions, shown in Figures 4, 5 and 6, give information about the viscous character of

the suspensions which cannot be obtained from viscosity measurements alone. As may be seen from the figures, all of these suspensions are essentially Newtonian fluids at low concentrations, i.e., the rate of shear is directly proportional to the shearing stress. The water-No. 18 glass suspensions appear to become somewhat dilatant at higher concentrations and the apparent viscosity increases with increasing shearing stress. Quicksand is another example of a dilatant suspension. This departure from a straight line may be caused by the introduction of turbulence as discussed below, although the break is usually more pronounced when due to turbulence. The water-attaclay and the water-graphite suspensions become less viscous with increasing shearing stress at the higher concentrations. It is not apparent from the data whether these latter suspensions are Bingham plastics or pseudoplastics. A Bingham plastic gives a positive intercept on the shear stress axis, while a pseudoplastic gives a curve coming to the origin. Absolute distinction cannot be made between the two types for these two suspensions because there are not enough points at low rates of shear to establish the lower portions of the shear diagrams accurately.

As may be seen from the shear diagrams, the slopes of the curves decrease rapidly at a Reynolds number of about 1500. Alves (1949) shows that this behavior is typical of turbulent flow. This is taken to mean that at this condition the suspensions began to flow turbulently. A critical Reynolds number of 1500 is lower than usually found. It probably results from the fact that the stirring required to keep the particles in suspension induced extra turbulence.

Correlation of Results.--The substitution of the geometric standard deviation for the constant k in Equation 14 gave reasonably good results as is shown in Figures 11 through 14. The maximum deviation of the experimental points from the calculated lines was obtained with the most concentrated solutions. The water-graphite solution containing 16.00 volume per cent solids was in error by approximately sixty per cent and the water-attaclay suspension containing 14.00 volume per cent was in error by about seventy per cent. All other points deviated less than fifty per cent, with most of the points being much closer to the calculated value than this. The most obvious exception to this fact is the series of runs with the water-No. 9 glass spheres. The experimental points for this suspension are thirty to forty per cent below the calculated values, and a line through the points, when extrapolated to zero concentration, does not give a relative viscosity of unity as do all other suspensions. There are two factors which contribute to this result and both are due to the particle size. Since the particles are large they have a fairly high settling velocity and tend to settle in the viscometer chamber. The result is that the concentration in the capillary is higher than the average value in the viscometer chamber and a lower relative viscosity is obtained. The other effect is the slippage of particles along the smooth walls when the particle size is large compared to the diameter of the capillary. Vand (1948) has analyzed this situation and found that the true viscosity is less than that indicated by a capillary viscometer. Since the true viscosity should be lower, the relative viscosity should be higher than that indicated by the points.

As may be seen from Figure 10, for a monodisperse suspension, i.e., one with particles having a geometric standard deviation of unity, Equation 15 reduces to Equation 6. No viscosity measurements on purely monodisperse suspensions are known to the author. However, Robinson (1951) obtained viscosity and settling volume data on three sized fractions of glass spheres. The spheres were seperated by repeated sedimentation into the size ranges 3 to 4 microns, 4 to 10 microns and 10 to 30 microns. No size distributions were obtained for these beads, but based solely on the nominal maximum and minimum size in each range, the geometric standard deviation of successive sized fractions would be larger, and it would be expected that k would be progressively larger for each fraction. This is indeed the case; values of k of 1.53, 1.76 and 1.92, respectively, were obtained for the three sized fractions.

While Equation 15 leaves much to be desired in the prediction of the viscosity of solid-liquid suspensions, it should be remembered that none of the constants in this equation need to be determined from viscosity measurements. All of the constants can be determined in most cases from easily measured or from previously determined physical properties of the solid and liquid components.

If a more extensive survey of viscosity characteristics is warranted, the use of Equation 14, where k is determined experimentally, gives much more accurate results.

CHAPTER VI

CONCLUSIONS

As a result of the work reported in this investigation the following conclusions may be drawn:

1. The viscosity of solid-liquid suspensions may be predicted with moderate accuracy for suspensions which are approximately Newtonian, i.e., those with nearly linear shear diagrams, by means of the empirical relationship

$$\mu_o/\mu = (1 - C/C_s)^{\sigma}$$

without recourse to experimental viscosity measurements. All of the constants in this equation can be determined from easily-measured or from well-known physical properties of the solid and liquid components.

2. A more accurate indication of viscosity may be obtained by the use of the equation

$$\mu_o/\mu = (1 - C/C_s)^{k} ,$$

where k is determined from one or more experimental viscosity measurements.

APPENDIX

Table 1. Experimental Calibration and Viscosity Data.

Run No.	Fluid System	Volume of Solids in Fluid System (%)	Diameter of Capillary (mm.)	Temperature of Fluid System (° C.)	Density of Fluid System (g./ml.)	Time of Efflux (min.)	Vacuum Applied to Flask (mm. Hg)
1	Water	0	1.047	30.1	0.9957	2.134	0
2	Water	0	1.047	30.1	0.9957	2.144	0
3	Water	0	1.047	38.0	0.9930	1.850	0
4	Water	0	1.047	38.0	0.9930	1.845	0
5	Water	0	1.047	50.0	0.9881	1.553	0
6	Water	0	1.047	50.0	0.9881	1.558	0
7	Water	0	1.047	60.0	0.9832	1.377	0
8	Water	0	1.339	30.2	0.9956	0.917	0
9	Water	0	1.339	30.0	0.9957	0.919	0
10	Water	0	1.339	36.0	0.9940	0.838	0
11	Water	0	1.339	36.0	0.9940	6.023	-4.23
12	Water	0	1.339	36.0	0.9940	2.047	-2.96
13	Water	0	1.339	36.0	0.9940	1.173	-1.53
14	Water	0	1.339	36.0	0.9940	0.610	2.37
15	Water	0	1.339	36.0	0.9940	0.532	4.60
16	Water	0	1.339	36.0	0.9940	0.490	6.63
17	Water	0	1.339	36.0	0.9940	0.467	8.75
18	Ethylene Glycol	0	1.339	36.0	1.102	25.05	0
19	Ethylene Glycol	0	1.339	50.0	1.012	15.93	0
20	Water-15.62% Glycerine	0	1.047	30.0	1.0360	3.001	0
21	Water-15.62% Glycerine	0	1.047	30.0	1.0360	3.001	0
22	Water-15.62% Glycerine	0	1.339	30.2	1.0333	1.253	0
23	Water-15.62% Glycerine	0	1.339	30.0	1.0360	1.257	0
24	Water-31.53% Glycerine	0	1.339	30.0	1.0740	1.927	0
25	Water-31.53% Glycerine	0	1.339	30.0	1.0740	1.927	0
26	Water-Graphite	16.68	1.047	83.0	1.169	12.150	0

(Continued)

Table 1 (Continued). Experimental Calibration and Viscosity Data.

Run No.	Fluid System	Volume of Solids in Fluid System (%)	Diameter of Capillary (mm.)	Temperature of Fluid System (° C.)	Density of Fluid System (g./ml.)	Time of Efflux (min.)	Vacuum Applied to Flask (mm. Hg)
27	Water-Graphite	16.00	1.339	36.0	1.154	13.497	0
28	Water-Graphite	16.00	1.339	36.0	1.154	2.030	11.43
29	Water-Graphite	16.00	1.339	36.0	1.154	1.520	14.98
30	Water-Graphite	16.00	1.339	36.0	1.154	1.130	19.49
31	Water-Graphite	16.00	1.339	36.0	1.154	0.670	31.94
32	Water-Graphite	13.82	1.047	81.6	1.141	5.428	0
33	Water-Graphite	13.77	1.047	86.5	1.141	5.303	0
34	Water-Graphite	13.00	1.339	36.0	1.123	4.217	0
35	Water-Graphite	13.00	1.339	36.0	1.123	1.830	3.54
36	Water-Graphite	13.00	1.339	36.0	1.123	1.100	7.59
37	Water-Graphite	13.00	1.339	36.0	1.123	0.697	13.44
38	Water-Graphite	12.00	1.339	36.0	1.105	3.653	0
39	Water-Graphite	12.00	1.339	36.0	1.105	1.290	4.21
40	Water-Graphite	12.00	1.339	36.0	1.105	0.973	7.60
41	Water-Graphite	12.00	1.339	36.0	1.105	0.657	11.37
42	Water-Graphite	12.00	1.339	36.0	1.105	0.660	11.81
43	Water-Graphite	10.79	1.047	79.5	1.069	3.370	0
44	Water-Graphite	10.79	1.047	79.5	1.069	2.882	0
45	Water-Graphite	10.79	1.047	79.5	1.069	3.223	0
46	Water-Graphite	10.79	1.047	79.5	1.069	3.057	0
47	Water-Graphite	10.78	1.047	83.1	1.066	2.871	0
48	Water-Graphite	10.78	1.047	83.1	1.066	2.996	0
49	Water-Graphite	9.25	1.047	30.0	1.090	4.378	0
50	Water-Graphite	9.22	1.047	38.0	1.084	3.638	0
51	Water-Graphite	9.12	1.047	60.0	1.075	2.607	0
52	Water-Graphite	9.03	1.047	83.5	1.058	2.256	0

(Continued)

Table 1 (Continued). Experimental Calibration and Viscosity Data.

Run No.	Fluid System	Volume of Solids in Fluid System (%)	Diameter of Capillary (mm.)	Temperature of Fluid System (° C.)	Density of Fluid System (g./ml.)	Time of Efflux (min.)	Vacuum Applied to Flask (mm. Hg)
53	Water-Graphite	9.03	1.047	83.5	1.058	2.050	0
54	Water-Graphite	9.01	1.047	86.5	1.056	2.091	0
55	Water-Graphite	9.01	1.047	86.5	1.056	2.120	0
56	Water-Graphite	8.00	1.339	36.0	1.073	2.256	0
57	Water-Graphite	8.00	1.339	36.0	1.073	1.080	3.62
58	Water-Graphite	8.00	1.339	36.0	1.073	0.777	6.25
59	Water-Graphite	8.00	1.339	36.0	1.073	0.670	8.05
60	Water-Graphite	8.00	1.339	36.0	1.073	0.553	10.85
61	Water-Graphite	8.00	1.339	36.0	1.073	0.423	15.30
62	Water-Graphite	6.98	1.047	77.2	1.042	1.906	0
63	Water-Graphite	4.74	1.047	75.7	1.020	1.543	0
64	Water-Graphite	4.74	1.047	79.5	1.017	1.480	0
65	Water-Graphite	4.73	1.047	86.4	1.014	1.398	0
66	Water-Graphite	4.00	1.339	36.0	1.033	1.107	0
67	Water-Graphite	4.00	1.339	36.0	1.033	0.743	2.45
68	Water-Graphite	4.00	1.339	36.0	1.033	0.587	4.83
69	Water-Graphite	4.00	1.339	36.0	1.033	0.500	8.15
70	Water-Graphite	2.00	1.047	72.3	0.997	1.375	0
71	Water-Graphite	2.00	1.047	72.4	0.997	1.383	0
72	Water-Graphite	1.89	1.047	73.3	0.996	1.370	0
73	Water-Attaclay	14.00	1.339	36.0	1.209	6.630	0
74	Water-Attaclay	14.00	1.339	36.0	1.209	1.747	12.2
75	Water-Attaclay	14.00	1.339	36.0	1.209	1.230	23.2
76	Water-Attaclay	14.00	1.339	36.0	1.209	0.830	30.4
77	Water-Attaclay	14.00	1.339	36.0	1.209	0.607	42.2
78	Water-Attaclay	12.46	1.047	36.0	1.186	11.207	0

(Continued)

Table 1 (Continued). Experimental Calibration and Viscosity Data.

Run No.	Fluid System	Volume of Solids in Fluid System (%)	Diameter of Capillary (mm.)	Temperature of Fluid System (° C.)	Density of Fluid System (g./ml.)	Time of Efflux (min.)	Vacuum Applied to Flask (mm. Hg)
79	Water-Attaclay	10.90	1.047	36.0	1.162	8.303	0
80	Water-Attaclay	10.26	1.339	36.0	1.152	2.733	0
81	Water-Attaclay	10.26	1.339	36.0	1.152	0.680	13.4
82	Water-Attaclay	10.26	1.339	36.0	1.152	0.430	24.2
83	Water-Attaclay	10.26	1.339	36.0	1.152	0.337	34.0
84	Water-Attaclay	9.86	1.339	36.0	1.146	2.233	0
85	Water-Attaclay	9.09	1.047	36.0	1.133	5.413	0
86	Water-Attaclay	8.01	1.339	36.0	1.117	1.701	0
87	Water-Attaclay	8.01	1.339	36.0	1.117	0.617	15.4
88	Water-Attaclay	8.01	1.339	36.0	1.117	0.480	21.0
89	Water-Attaclay	8.01	1.339	36.0	1.117	0.407	26.9
90	Water-Attaclay	7.59	1.047	36.0	1.109	4.190	0
91	Water-Attaclay	7.25	1.339	36.0	1.105	1.520	0
92	Water-Attaclay	6.00	1.047	36.0	1.086	3.413	0
93	Water-Attaclay	5.50	1.339	36.0	1.078	1.310	0
94	Water-Attaclay	5.50	1.339	36.0	1.078	0.440	10.2
95	Water-Attaclay	5.50	1.339	36.0	1.078	0.413	15.2
96	Water-Attaclay	5.50	1.339	36.0	1.078	0.380	20.0
97	Water-Attaclay	5.50	1.339	36.0	1.078	0.363	22.3
98	Water-Attaclay	4.24	1.047	36.0	1.059	2.667	0
99	Water-Attaclay	4.13	1.339	36.0	1.057	1.110	0
100	Water-Attaclay	3.32	1.047	36.0	1.045	2.460	0
101	Water-Attaclay	3.03	1.339	36.0	1.040	1.027	0
102	Water-Attaclay	2.46	1.047	36.0	1.032	2.270	0
103	Water-Attaclay	2.22	1.339	36.0	1.028	0.970	0
104	Water-Attaclay	1.74	1.047	36.0	1.021	2.180	0

(Continued)

Table 1 (Continued). Experimental Calibration and Viscosity Data.

Run No.	Fluid System	Volume of Solids in Fluid System (%)	Diameter of Capillary (mm.)	Temperature of Fluid System (° C.)	Density of Fluid System (g./ml.)	Time of Efflux (min.)	Vacuum Applied to Flask (mm. Hg)
105	Water-Attaclay	0.868	1.047	36.0	1.008	2.043	0
106	Water-No. 18 Glass	30.00	1.339	36.0	1.553	1.382	0
107	Water-No. 18 Glass	30.00	1.339	36.0	1.553	0.880	4.82
108	Water-No. 18 Glass	30.00	1.339	36.0	1.553	0.717	8.08
109	Water-No. 18 Glass	30.00	1.339	36.0	1.553	0.573	12.85
110	Water-No. 18 Glass	20.00	1.339	36.0	1.368	1.110	0
111	Water-No. 18 Glass	20.00	1.339	36.0	1.368	0,890	1.66
112	Water-No. 18 Glass	20.00	1.339	36.0	1.368	0.770	3.25
113	Water-No. 18 Glass	20.00	1.339	36.0	1.368	0.617	5.90
114	Water-No. 18 Glass	20.00	1.339	36.0	1.368	0.560	8.03
115	Water-No. 18 Glass	20.00	1.339	36.0	1.368	0.477	10.40
116	Water-No. 18 Glass	15.00	1.339	36.0	1.274	1.023	0
117	Water-No. 18 Glass	13.08	1.339	36.1	1.237	0.990	0
118	Water-No. 18 Glass	10.00	1.339	36.0	1.180	0.967	0
119	Water-No. 18 Glass	10.00	1.339	36.0	1.180	0.953	0.11
120	Water-No. 18 Glass	10.00	1.339	36.0	1.180	0.770	1.65
121	Water-No. 18 Glass	10.00	1.339	36.0	1.180	0.647	3.35
122	Water-No. 18 Glass	10.00	1.339	36.0	1.180	0.587	5.16
123	Water-No. 18 Glass	10.00	1.339	36.0	1.180	0.557	7.18
124	Water-No. 18 Glass	5.00	1.339	36.0	1.087	0.917	0
125	Water-No. 18 Glass	5.00	1.339	36.0	1.087	1.630	-2.00
126	Water-No. 18 Glass	5.00	1.339	36.0	1.087	0.730	1.73
127	Water-No. 18 Glass	5.00	1.339	36.0	1.087	0.680	3.00
128	Water-No. 18 Glass	5.00	1.339	36.0	1.087	0.620	4.86
129	Water-No. 9 Glass	21.56	1.339	36.0	1.394	1.490	0
130	Water-No. 9 Glass	16.60	1.339	36.0	1.304	1.340	0

(Continued)

Table 1 (Concluded). Experimental Calibration and Viscosity Data.

Run No.	Fluid System	Volume of Solids in Fluid System (%)	Diameter of Capillary (mm.)	Temperature of Fluid System (° C.)	Density of Fluid System (g./ml.)	Time of Efflux (min.)	Vacuum Applied to Flask (mm. Hg)
131	Water-No. 9 Glass	9.40	1.339	36.0	1.169	1.210	0
132	Water-No. 9 Glass	1.20	1.339	36.0	1.036	1.070	0
133	Water-Aluminum	5.30	1.339	36.0	1.072	2.020	0
134	Water-Aluminum	3.25	1.339	36.0	1.047	1.770	0
135	Water-Aluminum	2.10	1.339	36.0	1.026	1.333	0
136	Water-Copper	19.05	1.047	36.0	2.373	2.597	0
137	Water-Copper	17.00	1.047	36.0	2.223	2.313	0
138	Water-Copper	14.99	1.339	36.0	2.080	0.983	0
139	Water-Copper	12.47	1.047	36.0	1.899	1.987	0
140	Water-Copper	11.00	1.339	36.1	1.788	0.887	0
141	Water-Copper	10.79	1.047	36.0	1.775	1.873	0
142	Water-Copper	9.15	1.047	36.0	1.655	1.873	0
143	Water-Copper	8.08	1.339	36.0	1.580	0.837	0
144	Water-Copper	7.92	1.047	36.0	1.566	1.880	0
145	Water-Copper	6.70	1.047	36.0	1.477	1.860	0
146	Water-Copper	5.00	1.047	36.0	1.356	1.883	0
147	Water-Copper	4.60	1.339	36.0	1.325	0.833	0
148	Water-Copper	3.35	1.047	36.0	1.232	1.897	0
149	Ethylene Glycol-Graphite	20.0	1.339	50.0	1.516	216.27	0
150	Ethylene Glycol-Graphite	13.03	1.339	50.0	1.289	38.13	0
151	Ethylene Glycol-Graphite	7.41	1.339	50.0	1.198	20.98	0
152	Ethylene Glycol-Aluminum	3.18	1.339	36.0	1.161	46.27	0
153	Ethylene Glycol-Aluminum	2.10	1.339	36.0	1.143	35.78	0

Table 2. Constant Properties of Fluid Systems.

Fluid System	Density of Particles (g./ml.)	Median Particle Size (microns)	Standard Deviation	Value of k in Equation 14	Volume of Solids in Settled Bed (%)
Water-Graphite	1.99	4.41	2.26	2.38	26.4
Water-Attaclay	2.535	1.20	1.98	1.72	18.2
Water-No. 18 Glass	2.86	35.0	1.42	1.26	51.0
Water-No. 9 Glass	2.86	260	1.27	1.48	60.2
Water-Aluminum	2.70	10.2	2.45	2.32	12.1
Water-Copper	8.23	3.20	2.28	2.64	54.1
Ethylene Glycol-Graphite	1.99	4.41	2.26	2.03	27.6
Ethylene Glycol-Aluminum	2.70	10.2	2.45	1.54	8.9

Table 3. Calibration of Instrument Constants from Equation 12.*

Calculated from Runs No.	Capillary Diameter (mm.)	ν, Kinematic Viscosity (centistoke)	t, Time of Efflux (min.)	νt (centistoke-min.)	t^2 ($min.^2$)
1, 2	1.047	0.8024	2.138	1.715	4.571
3, 4	1.047	0.6826	1.850	1.269	3.422
5, 6	1.047	0.5560	1.555	0.865	2.418
7	1.047	0.4768	1.377	0.657	1.896
20, 21	1.047	1.153	3.001	3.460	9.006
8, 9	1.339	0.9956	0.803	0.736	0.845
10	1.339	0.7120	0.838	0.597	0.702
22, 23	1.339	1.154	1.255	1.447	1.575
24, 25	1.339	1.979	1.927	3.551	3.713

*For 1.047 mm. Capillary, a = 0.3948 and b = 0.092.
For 0.339 mm. Capillary, a = 0.9800 and b = 0.092.

Table 4. Calculated Values of Viscosity and Related Functions.

Calculated from Runs No.	Reduced Volume of Solids	Viscosity (centipoise)	Reduced Viscosity	$1 - C/C_s$
26	0.638	5.60	0.064	0.362
27	0.606	15.54	0.046	0.394
32	0.524	2.427	0.148	0.474
33	0.521	2.369	0.144	0.479
34	0.492	4.713	0.150	0.508
38	0.455	3.860	0.183	0.545
43, 46	0.409	1.388	0.266	0.591
47, 48	0.408	1.241	0.286	0.592
49	0.350	1.862	0.434	0.620
50	0.349	1.532	0.442	0.651
51	0.346	1.070	0.433	0.654
52, 53	0.342	0.853	0.414	0.658
54, 55	0.342	0.832	0.412	0.658
56	0.303	2.327	0.304	0.697
62	0.264	0.754	0.498	0.736
63	0.180	0.576	0.665	0.820
64	0.179	0.547	0.674	0.821
65	0.179	0.509	0.674	0.821
66	0.151	1.034	0.684	0.849
70, 71	0.076	0.476	0.840	0.924
72	0.072	0.472	0.835	0.928
73	0.770	7.85	0.090	0.230
78	0.685	5.249	0.135	0.315
79	0.599	3.797	0.186	0.401
80	0.564	3.060	0.231	0.436
84	0.542	2.460	0.288	0.458
85	0.499	2.402	0.294	0.501
86	0.440	1.803	0.392	0.560
90	0.427	1.812	0.391	0.573
91	0.399	1.582	0.447	0.601
92	0.330	1.434	0.493	0.670
93	0.302	1.308	0.541	0.698
98	0.232	0.976	0.725	0.768
99	0.227	1.063	0.665	0.773
100	0.177	0.976	0.725	0.823
101	0.166	0.954	0.741	0.834
102	0.135	0.882	0.802	0.865
103	0.122	0.882	0.802	0.878
104	0.095	0.836	0.845	0.905
105	0.048	0.768	0.921	0.952

(Continued)

Table 4 (Concluded). Calculated Values of Viscosity and Related Functions.

Calculated from Runs No.	Reduced Volume of Solids	Viscosity (centipoise)	Reduced Viscosity	$1 - C/C_s$
106	0.588	2.005	0.353	0.412
110	0.392	0.450	0.488	0.608
116	0.294	1.163	0.608	0.705
117	0.256	1.085	0.652	0.744
118	0.196	1.006	0.704	0.804
124	0.098	0.869	0.814	0.902
129	0.358	1.947	0.363	0.642
130	0.276	1.623	0.436	0.724
131	0.156	1.296	0.546	0.844
132	0.020	0.996	0.710	0.980
133	0.438	2.084	0.339	0.672
134	0.269	1.761	0.402	0.731
135	0.174	1.298	0.545	0.825
136	0.352	2.349	0.301	0.648
137	0.314	1.942	0.364	0.686
138	0.277	1.810	0.391	0.723
139	0.231	1.395	0.506	0.769
140	0.204	1.368	0.517	0.796
141	0.200	1.230	0.575	0.800
142	0.169	1.143	0.618	0.831
143	0.149	1.122	0.630	0.851
144	0.146	1.086	0.652	0.854
145	0.124	1.010	0.700	0.876
146	0.092	0.942	0.750	0.908
147	0.085	0.936	0.755	0.915
148	0.062	0.863	0.820	0.938
149	0.725	134.1	0.052	0.275
150	0.471	20.11	0.348	0.529
151	0.268	10.28	0.681	0.732
152	0.357	21.97	0.505	0.643
153	0.236	16.72	0.664	0.764

Table 5. Calculated Values of Points on Shear Diagrams.

Calculated from Run No.	Mean Pressure Drop through Viscometer ($g_f./cm.^2$)	Shear Stress ($g_f./cm.^2$)	Rate of Shear ($g_f.sec./g.cm.$)
11	11	0.005	0.96
12	28	0.015	1.89
13	47	0.025	3.30
10	67	0.035	4.61
14	100	0.052	6.34
15	130	0.068	7.27
16	158	0.082	7.84
17	186	0.097	8.29
27	79	0.041	0.28
28	234	0.122	1.91
29	282	0.147	2.54
30	343	0.178	3.42
31	512	0.266	5.76
34	77	0.040	0.92
35	125	0.065	2.11
36	179	0.093	3.52
37	259	0.135	5.55
38	75	0.039	1.06
39	132	0.069	3.00
40	178	0.093	4.04
41	230	0.120	5.89
42	236	0.123	5.86
56	73	0.038	1.85
57	122	0.064	3.58
58	158	0.082	4.98
59	182	0.095	5.77
60	220	0.114	6.99
61	280	0.146	9.14
66	71	0.037	3.49
67	104	0.054	5.20
68	136	0.071	6.60
69	181	0.094	7.74
73	81	0.042	0.58
74	249	0.129	2.21
75	397	0.206	3.14
76	495	0.257	4.66
77	654	0.340	6.37
80	77	0.040	1.41
81	261	0.136	5.69

(Continued)

Table 5 (Concluded). Calculated Values of Points on Shear Diagrams.

Calculated from Run No.	Mean Pressure Drop through Viscometer ($g_f./cm.^2$)	Shear Stress ($g_f./cm.^2$)	Rate of Shear ($g_f.sec./g.cm.$)
82	407	0.212	9.00
83	539	0.280	11.49
86	75	0.039	2.28
87	284	0.148	6.27
88	360	0.187	8.06
89	439	0.228	9.51
93	72	0.037	2.95
94	210	0.109	8.79
95	280	0.146	9.35
96	347	0.180	10.18
97	376	0.196	10.63
106	104	0.054	2.79
107	171	0.089	4.40
108	215	0.112	5.40
109	280	0.145	6.74
110	92	0.048	3.48
111	116	0.060	4.52
112	138	0.072	5.02
113	173	0.090	6.27
114	202	0.105	7.16
115	234	0.122	8.11
118	79	0.041	4.00
119	81	0.042	4.06
120	102	0.053	5.02
121	126	0.065	5.98
122	148	0.077	6.60
123	178	0.092	6.95
125	48	0.025	2.70
124	73	0.038	4.22
126	98	0.051	5.30
127	115	0.060	5.69
128	140	0.073	6.23

Table 6. Calculated Values for Lines of Constant Reynolds Number on Shear Diagrams.

Fluid System	Reynolds Number	Volume of Solids in Fluid System (%)	Apparent Viscosity (centipoise)	Rate of Shear (gf.sec./g.cm.)
Water	1500	0	0.707	4.68
Water	1000	0	0.707	3.24
Water	500	0	0.707	1.62
Water-Graphite	1500	4.00	1.055	6.97
Water-Graphite	1500	8.00	1.580	10.04
Water-Graphite	1500	12.00	1.909	11.28
Water-Graphite	1000	4.00	1.055	4.65
Water-Graphite	1000	8.00	1.621	6.87
Water-Graphite	1000	12.00	1.974	8.12
Water-Graphite	1000	13.00	2.273	9.20
Water-Graphite	500	4.00	1.055	2.55
Water-Graphite	500	8.00	1.749	3.71
Water-Graphite	500	12.00	2.175	4.49
Water-Graphite	500	13.00	2.476	5.02
Water-Attaclay	1500	5.50	1.259	7.98
Water-Attaclay	1500	10.26	2.440	13.95
Water-Attaclay	1000	5.50	1.259	4.24
Water-Attaclay	1000	10.26	2.353	5.25
Water-Attaclay	500	5.50	1.259	2.66
Water-Attaclay	500	10.26	2.430	4.81
Water-Attaclay	500	14.00	5.370	10.26
Water-No. 18 Glass	1500	5.00	0.938	5.89
Water-No. 18 Glass	1500	10.00	1.050	6.07
Water-No. 18 Glass	1500	20.00	1.412	7.05
Water-No. 18 Glass	1000	5.00	0.938	3.92
Water-No. 18 Glass	1000	10.00	1.050	4.05
Water-No. 18 Glass	1000	20.00	1.412	4.70
Water-No. 18 Glass	1000	30.00	2.000	5.86
Water-No. 18 Glass	500	5.00	0.938	1.97
Water-No. 18 Glass	500	10.00	1.050	2.03
Water-No. 18 Glass	500	20.00	1.412	2.35
Water-No. 18 Glass	500	30.00	2.000	2.94

Table 7. Miscellaneous Information on Suspension Materials.

Material	Information
Graphite	Acheson graphite, manufactured by National Carbon Company, Niagra Falls, N. Y. 98.5 weight per cent through 200-mesh screen.
Attaclay	Attapulgus clay, refined by the Attapulgus Clay Company, Philadelphia 5, Pa.
No. 18 Glass	Glass spheres manufactured by the Minnesota Mining and Manufacturing Company, Saint Paul, Minn.
No. 9 Glass	Same as No. 18 Glass except larger spheres.
Copper	Copper powder supplied by A. C. Mackay, 198 Broadway, New York, N. Y.
Aluminum	Aluminum powder manufactured by the Aluminum Company of America, Pittsburg, Pa. Five weight per cent retained on 100-mesh screen, 75 weight per cent passed through 325-mesh screen.

DERIVATION OF POISEUILLE'S LAW AND THE MEAN LOGARITHMIC HEAD

Derivations of Poiseuille's law may be found in many textbooks. The following derivation of this law and of the mean logarithmic head are essentially the same as those used by Orr (1952) and the credit is due to him for the arrangement used.

Sir Isaac Newton defined the coefficient of viscosity of an ideal liquid as the numerical value of the tangential force on a unit area of one of two parallel planes a unit distance apart when the space between the planes is filled with the liquid in question and one of the planes moves with unit velocity in its own plane relative to the other. Expressed mathematically, this is

$$F = \mu v/x \quad , \tag{17}$$

where F is the force, v is the velocity, x is the distance of separation, and μ is called the coefficient of viscosity. Since the velocity of the liquid changes continuously, this equation may be written with differentials as

$$F = \mu \, dv/dx \quad . \tag{18}$$

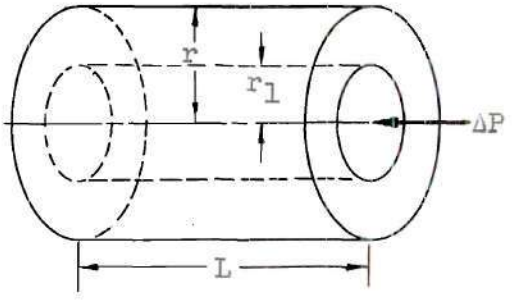

Consideration of this equation and of the conditions imposed when a liquid flows through a tube permits the derivation of a readily usable expression. With the tube horizontal

so that the weight of the liquid is of no influence, let pressures be applied to both ends of the tube such that a net pressure, ΔP, is exerted as shown in the sketch on the previous page. If the liquid was originally at rest, it will move with ever-increasing velocity until the viscous resistance just balances the driving pressure. The condition for equilibrium may be written for the liquid cylinder of length L and radius r_1. The cross-sectional area of the cylinder is πr_1^2, and if ΔP is the pressure per unit area, the driving force is $\pi r_1^2 \Delta P$. The viscous resistance, F per unit area, acts on the sides of the cylinder of area $2\pi r_1 L$ with a total force of $2\pi r_1 LF$. Since equilibrium conditions prevail,

$$2\pi r_1 LF = \pi r_1^2 \Delta P \quad , \tag{19}$$

or

$$F = r_1 \Delta P / 2L \quad .$$

Therefore, using Equation 18,

$$dv = \Delta P r_1 \, dr_1 / 2L\mu \quad . \tag{20}$$

Equation 20 may be integrated, yielding

$$v = \Delta P r_1^2 / 4L\mu + c \quad . \tag{21}$$

It has been found that, without exception, an ideal (or Newtonian) liquid adheres to the wall so that no slipping occurs; v is therefore zero when $r_1 = r$, and

$$v = \Delta P (r^2 - r_1^2) / 4L\mu \quad . \tag{22}$$

The velocity distribution, therefore, follows a parabola. As may be seen, dv/dr_1 vanishes for $r_1 = 0$, meaning that the parabola has a tangent normal to the axis there and that there is, furthermore, no cusp, corner, etc., at that point.

The maximum velocity at the center of the tube ($r_1 = 0$) is

$$v_{max} = \Delta P r^2 / 4L\mu \quad . \tag{23}$$

The volume of flow in a certain time is more convenient to use than the velocity of flow; therefore, by the well-known formula for the volume of a rotational paraboloid, the two quantities are related by

$$V/t = \pi r^2 v_{max} / 2 \quad . \tag{24}$$

Combining these last two equations results in the relationship which is known as Poiseuille's law,

$$V = \pi r^4 \Delta P t / 8L\mu \quad . \tag{25}$$

Poiseuille's law was derived so that an important point might be brought out. As discussed in the text, Poiseuille's law may be written as

$$\mu = \frac{g_c D}{8v} \cdot \frac{D\Delta P}{4L} \quad . \tag{26}$$

The last term, $D\Delta P / 4L$, may be seen by Equation 19 to be nothing but the shearing stress at the internal surface of the tube. The term $g_c D / 8v$ is therefore the rate of shear at the same place.

If P is expressed as the effective head causing the flow in the viscometer, Equation 25 may be expressed as

$$H = 128\mu LV/\pi\rho g_c D^4 t \quad . \tag{27}$$

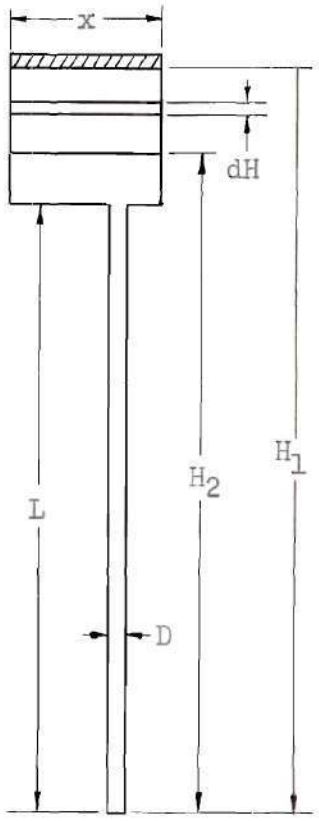

By referring to the accompanying sketch, it may be seen that

$$dV = -\frac{x^2\pi}{4} dH \quad , \tag{28}$$

and that, therefore, upon substituting Equation 28 into Equation 27 the relationship

$$\int_{H_2}^{H_1} \frac{dH}{H} = -\int_o^t \frac{\pi\rho D^4 g \, dt}{32 \, \mu x^2 \pi L} \tag{29}$$

is obtained, which, upon integration, becomes

$$\ln(H_1/H_2) = -\rho D^4 gt/32\mu x^2 L \tag{30}$$
$$= \frac{\rho D^4 gt}{128\mu V} \cdot \frac{4V}{x^2 L} \quad .$$

Equation 30 may be rearranged to give

$$\frac{4V}{x^2\pi \ln(H_1/H_2)} = \frac{128\mu LV}{\pi\rho g D^4 t} \quad . \tag{31}$$

From Equations 27 and 31 it may be seen that

$$H = \frac{4V}{x^2\pi \ln(H_1/H_2)} \quad , \tag{32}$$

while, from Equation 28, if it is integrated between the limits of $V = 0$ to $V = V$ and $H = H_1$ to $H = H_2$, it is evident that

$$V = x^2\pi(H_1 - H_2)/4 \quad . \tag{33}$$

Combining Equations 32 and 33, the result that

$$H = \frac{H_1 - H_2}{\ln(H_1/H_2)} \tag{34}$$

is obtained. This is the value of the logarithmic mean head.

NOMENCLATURE

a	constant
b	constant
C	fraction of volume occupied by solid particles
C_o	fraction of volume occupied by solid particles at "zero fluidity"
C_s	fraction of volume of a sedimented bed occupied by solid particles
C.	Centigrade
cm.	centimeters
D	diameter of capillary
d	constant
F	force
g	acceleration of gravity
g_c	conversion factor
g.	grams
g_f.	grams force
H	effective head of fluid
H_1	head of fluid at beginning of determination
H_2	head of fluid at end of determination
Hg	mercury
k	constant
L	length of capillary
m	constant
ml.	milliliters

mm.	millimeters
No.	number
pp.	pages
Re	Reynolds number
r	radius of capillary
r_1	distance from center of capillary
S	volume of sedimented bed per unit volume of solid particles
sec.	seconds
t	time
V	volume
v	velocity
v_{max}	maximum velocity
x	distance
ΔP	pressure drop
μ	viscosity of fluid
μ_a	apparent viscosity of suspension
μ_o	viscosity of liquid phase of suspension
ν	kinematic viscosity of fluid
ρ	density of fluid
ρ_o	density of liquid phase of suspension

BIBLIOGRAPHY

ALVES, G. E.
1949. "Flow of Non-Newtonian Suspensions." Chemical Engineering 56, 107-109.

BINGHAM, E. C.
1922. Fluidity and Plasticity. McGraw-Hill Book Company, Inc., New York.

---- AND DURHAM, T. C.
1911. "The Viscosity and Fluidity of Suspensions of Finely-Divided Solids in Liquids." American Chemical Journal 46, 278-297.

BONILLA, C. F., GERVI, A., JR., COLVEN, T. J., JR. AND WANG, S. J.
1951. "Heat Transfer to Slurries in Pipes. Chalk and Water in Turbulent Flow." Preprint, Heat Transfer Symposium, Forty-Fourth Annual Meeting of the American Institute of Chemical Engineers, December.

CARBIDE AND CARBON CHEMICALS CORPORATION
1947. Glycols. New York.

CHEMICAL AND ENGINEERING NEWS
1952. "Absolute Viscosity of Water at 20° C. Changes Value." Vol. 30, 249.

DALLAVALLE, J. M.
1948. Micromeritics. Pitman Publishing Corporation, New York.

EINSTEIN, A.
1906. "Eine neue Bestimmung der Moleküldimensionen." Annalen der Physik 19, 289-306.
1911. "Berichtigung zu meiner Arbeit: Eine neue Bestimmung der Moleküldimensionen." Annalen der Physik 34, 591-592.

EIRICH, F., BUNZL, M. AND MARGARETHA, H.
1936. "Untersuchungen über die Viskosität von Kugelsuspensionen." Kolloid Zeitschrift 74, 276-285.

GUTH, E. AND SIMHA, R.
1936. "Untersuchungen über die Viskosität von Suspensionen und Lösungen. 3. Über die Viskosität von Kugelsuspension." Kolloid Zeitschrift 74, 266-275.

HAGENBACH, E.
1860. "Ueber die Bestimmung der Zähigkeit einer Flüssigkeit durch den Ausflufs aus Röhren." Annalen Der Physik und Chemie 109, 285-426.

HALL, H. T. AND FUOSS, R. M.
1951. "Empirical Analysis of Viscosity Data." The Journal of the American Chemical Society 73, 265-269.

HATSCHEK, EMIL
1913. "The General Theory of Viscosity of Two-Phase Systems." Transactions of the Faraday Society 9, 80-92.
1920. "Die Viskosität von Blutkörperchen-Suspensionen." Kolloid Zeitschrift 27, 163-165.

LANGE, N. A. (Editor)
1949. Handbook of Chemistry. Handbook Publishers, Inc., Sandusky, Ohio.

MCBAIN, J. W.
1950. Colloid Science. D. C. Heath and Company, Boston

NORTON, F. H., JOHNSON, A. L. AND LAWRENCE, W. G.
1944. "Fundamental Study of Clay: VI. Flow Properties of Kaolinite-Water Suspensions." The Journal of the American Ceramic Society 27, 149-164.

ORR, C., JR.
1952. The Transference of Heat between a Pipe Wall and a Liquid-Solid Suspension Flowing Turbulently inside the Pipe. The Thermal Conductivity and Viscosity of a Liquid-Solid Suspension. Thesis. Georgia Institute of Technology.

---- AND DALLAVALLE, J. M.
1954. "Heat-Transfer Properties of Liquid-Solid Suspensions." Heat Transfer - Research Studies for 1954. American Institute of Chemical Engineers, New York. pp. 29-45.

REINER, M.
1949. Deformation and Flow. K. K. Lewis and Co., Ltd., London.

ROBINSON, J. V.
1949. "The Viscosity of Suspensions of Spheres." The Journal of Physical and Colloid Chemistry 53, 1042-56.
1951. "The Viscosity of Suspensions of Spheres. II. The Effect of Sphere Diameter." The Journal of Physical and Colloid Chemistry 53, 455-64.

VAND, V.
1948. "Viscosity of Solutions and Suspensions. II. Experimental Determination of the Viscosity-Concentration Function of Spherical Suspensions." The Journal of Physical and Colloid Chemistry 52, 300-314.

WILBERFORCE, L. R.
1891. "On the Calculation of the Coefficient of Viscosity of a Liquid from its Rate of Flow Through a Capillary Tube." The Philosophical Magazine 31, 407-414.